

Isochrony in 3D radial potentials

From Michel Hénon ideas to isochrone relativity:
classification, interpretation and applications

Alicia Simon-Petit¹
Jérôme Perez¹
Guillaume Duval²

¹ Ensta ParisTech, Paris Saclay University, Applied Mathematics Laboratory, France

² INSA Rouen, Mathematics & Informatics Laboratory, France

May 1, 2018

Abstract

Revisiting and extending an old idea of Michel Hénon, we geometrically and algebraically characterize the whole set of isochrone potentials. Such potentials are fundamental in potential theory. They appear in spherically symmetrical systems formed by a large amount of charges (electrical or gravitational) of the same type considered in mean-field theory. Such potentials are defined by the fact that the radial period of a test charge in such potentials, provided that it exists, depends only on its energy and not on its angular momentum. Our characterization of the isochrone set is based on the action of a real affine subgroup on isochrone potentials related to parabolas in the \mathbb{R}^2 plane. Furthermore, any isochrone orbits are mapped onto associated Keplerian elliptic ones by a generalization of the Bohlin transformation. This mapping allows us to understand the isochrony property of a given potential as relative to the reference frame in which its parabola is represented. We detail this isochrone relativity in the special relativity formalism. We eventually exploit the completeness of our characterization and the relativity of isochrony to propose a deeper understanding of general symmetries such as Kepler's Third Law and Bertrand's theorem.

Contents

1	Introduction	3
2	The isochrone geometry	6
2.1	Hénon's parabola	6
2.2	General properties of isochrone parabolas	9
2.3	Classification of isochrone potentials	15
2.4	Some physical meaning of this classification	18
2.5	The affine group action on the Isochrone set	20
3	Isochrone orbits and isochrone transformations	23
3.1	Introduction and motivation	23
3.1.1	Isochrone orbits transformations	24
3.1.2	The bolst as the generalized Bohlin transformation	25
3.1.3	The bolst, a key to isochrony	30
3.2	Isochrone relativity	31
3.2.1	The ibolst Algebra	32
3.2.2	Lengths and spaces	33
3.2.3	Orbits relativity	34
3.2.4	Potentials relativity	40
3.2.5	Isochrone orbits construction	42
4	Applications	43
4.1	Physical properties of isochrone potentials	43
4.2	Period and precession of periastron for isochrones	45
4.3	Generalization of Kepler's Third Law	49
4.4	The Bertrand theorem	53
5	Conclusion	55
A	Isochrone characterization	57
B	Proof of a parabola property	57
C	Useful Lemmas	61
D	Isochrone integrals	62
D.1	Computation of $\mathcal{A}_r^{\text{ke}}$, $\mathcal{A}_r^{\text{ha}}$ and physical deduction of \mathcal{I}_1	63
D.2	Proof for the expression of \mathcal{I}_2	64

1 Introduction

Macroscopic properties of self-gravitating systems can be derived from the orbits of their components, e.g. stars. These orbits are designed by the potential – density pair $(\psi - \rho)$ involved in Poisson’s equation $\Delta\psi = 4\pi G\rho$. This pair forms a steady-state model for such astrophysical systems and there are essentially two ways to produce a physically relevant model — one depending on empirical input, the other on theoretical input.

By compiling observational data, one can look for the emergence of an *empirical* model. For example, consider de Vaucouleur’s law for elliptical galaxies in the middle of the twentieth century [40]. In that paper, the author remarks that the projection $I(R)$ of the luminosity onto the plane of the sky of elliptical galaxies varies as a function of an apparent distance R from the center as $I(R) \propto \exp(-R^{1/4})$. From $I(R)$, assuming a given mass–to–light ratio, one can build the mass density ρ of the system and, solving Poisson’s equation, obtain a gravitational potential for elliptical galaxies. This problem is generally ill-posed: as a matter of fact, after the projection, a lot of “good” potentials (Jaffe [22], Hernquist [21], Dehnen [11] or NFW [34]) produce $R^{1/4}$ -compatible luminosity profiles. Apart from this empirical property all these famous models are poorly justified physically.

The reverse approach is much less investigated. The mass density is a marginal velocity law of the one-particle distribution function f associated with a self-gravitating system. This function $f(t, \mathbf{r}, \mathbf{p})$ describes the statistical properties of a test particle of mass m , position \mathbf{r} and momentum \mathbf{p} in the mean field gravitational potential $\psi(t, \mathbf{r})$. These two functions satisfy the Collisionless-Boltzmann and Poisson system

$$\begin{cases} \frac{\partial f}{\partial t} + \{f, E\} = 0, \\ \Delta\psi = 4\pi G\rho = 4\pi mG \int f d\mathbf{p}, \end{cases}$$

where $E = \frac{\mathbf{p}^2}{2m} + m\psi$ is the total energy of the test particle and $\{, \}$ stands for the Poisson bracket. Using basic properties of these brackets, one can see that the simplest steady states are described by $f(E)$: this is the simplest case of Jeans’ theorem (see e.g. [6]). Involving Gidas-Nirenberg theorem [14], one can show ([35] sect. 2) that, if their total mass is finite, the corresponding self-gravitating systems are spherical and isotropic and thus their gravitational potentials are radial, $\psi = \psi(r)$ with $r = |\mathbf{r}|$. Stability analysis can restrict possible steady states to decreasing and positive f but nothing general can be said anymore about the choice of an equilibrium in this context. Adding thermodynamic considerations,

Lynden-Bell [28] has initiated a long debate. Based on the fact that in three spatial dimensions there is no regular isothermal steady states with finite mass, this debate is often summarized by the fact that isolated self-gravitating systems could settle down in a truncated isothermal state with a core-halo density distribution. The size of the core and the slope of the halo depend on structural dissipation which can occur in the system. This point will be discussed in a forthcoming paper.

In a singular and seminal paper in French, Hénon [20] (for an English translation see [5]) followed another way to address this problem. Radial potentials confer to any of their confined test particles the property to have a periodic radial distance from the center of the system. This radial period τ_r depends generically on the two physical parameters of this test particle: its energy E and the modulus L^2 of its squared angular momentum. Hénon remarks that orbits confined around the center of the system (which evolve generically in a harmonic potential) and orbits confined to the outer parts (which evolve generically in a Keplerian potential) have a radial period that depends only on E . He then proposed looking for a general potential which could be characterized by this property. He succeeded by finding his famous isochrone potential. Although his potential gives a mass density in pretty good accordance with some of the observed globular clusters at the time, history has decided to follow another direction. In his conclusion, Michel Hénon proposed a mechanism based on resonances that could lead to the formation of an isochrone. This mechanism needed to be considered more accurately and proved substantially [20, 5], but it has not been further investigated. In addition to Lynden-Bell's work on violent relaxation and the above-mentioned debate that followed, the observational data refinement and the development of numerical simulations revealed a great variety of profiles for self-gravitating systems and Hénon's isochrone became one among them. Recent works (in a paper in preparation by Simon-Petit, A., Perez, J, and Plum, G.) reveal that, as suggested by Hénon [20] in his conclusion, isochrony could in fact be inherited from the formation process of isolated self-gravitating systems. Hence there could be a fundamental initial state from which, after the initial collapse, the observed diversity could arise.

For all of these reasons, we have decided to revisit in detail isochrony in radial potential-governed systems. Inspecting Hénon ideas we have found that his work is far from exhaustive in a mathematical sense even if the potential he has found might be one of the most important for physical applications. We propose in this paper to characterize the whole set of isochrone potentials in a rigorous way. This characterization will help for a

global understanding of the importance of the isochrone property and will clarify some important physical symmetries occurring in gravitation like Kepler's Third law or Bertrand's theorem.

The paper is organized as follows. In the spirit of Michel Hénon, section 2 is devoted to geometry. In sec. 2.1 we first recall the basics of the problem of potential isochrony, general definitions and the Hénon link between isochrony and parabolas. In addition, we call for a rigorous proof of this parabola property which is given in appendix B. Taking into account very general physical properties, we introduce in sec. 2.2 appropriate transformations and prove three lemmas which allow us to restrict the study to parabolas passing through the origin with a vertical or a horizontal tangent. As these transformations leave invariant vertical lines, these three lemmas will make clear the decomposition of parabolas into four families: ones with a vertical symmetry axis (straight parabolas) and others (tilted parabolas) that are classified in three different types depending on the parabola orientation and vertical tangent position. These transformations and hence this distinction were not identified by Hénon who also missed some elements of the isochrone set. Thanks to this geometric decomposition, we deduce in sec. 2.3 the whole set of isochrone potentials. It is a modulus space in which each point is a potential from one of the four classes of equivalence of parabolas under the action of the previous transformations. This algebraic representation classifies the four isochrone potential types but separates them in a partition of four equivalence classes. However, isochrone potentials are unified, linking orbits together.

In section 3, we focus on the isochrone orbits. Based on the fundamental differential orbital equation, we present in sec. 3.1 the most general transformation which preserves isochrony and angular momentum when applied to a given orbit. This linear application is then identified as a generalization of the well-known Bohlin transformation ([7, 3]) as well as the brilliant idea of Donald Lynden-Bell [30]. It continuously maps isochrone orbits onto their Keplerian associates. This Keplerian character of a given isochrone orbit is developed in sec. 3.2. Adapting the time, energy and angular momentum of a given isochrone orbit in an isochrone potential, it is shown in detail how to map this orbit onto its associated Keplerian one in the appropriate frame.

The last section is devoted to physical applications of this isochrony classification and interpretation. We first present in sec. 4.1 the physical properties of systems associated with isochrone potentials. In particular, we give in table 50 the explicit formulation of $\tau_r(E)$ and $n_\varphi(L^2)$ for all isochrone potentials. The properties of $\tau_r(E)$ allow us to give a

generalization of Kepler’s third law in sec. 4.3. Eventually we show in sec. 4.4 that the famous Bertrand’s theorem about closed orbits in radial potentials is just a corollary of a general property of isochrone orbits.

Four appendices detail important results for isochrony used in the paper.

2 The isochrone geometry

2.1 Hénon’s parabola

We consider a stellar system described by a gravitational potential $\psi(\mathbf{r}) = \psi(r)$, where \mathbf{r} is the position vector of a test particle of mass m confined in this system. The orbit of this test particle is contained in a plane. In this plane, the two parameters of this orbit are its energy $E = m\xi$ and the norm of its angular momentum $L = m\Lambda$. Both these two parameters contribute to the definition of the gravitational potential of the cluster $\psi(r)$ and to the computation of the distance r between the star and the center of mass of the cluster at each time t . This contribution is summarized in the definition of the energy of the star,

$$\xi = \frac{1}{2} \left(\frac{dr}{dt} \right)^2 + \frac{\Lambda^2}{2r^2} + \psi(r) = \text{cst.} \quad (1)$$

We are interested in increasing¹ potentials $\psi(r)$ for which the ODE (1) admits periodic solutions, named hereafter Periodic Radial Orbits (PROs). The effective potential $\psi_e(r) = \frac{\Lambda^2}{2r^2} + \psi(r)$ then reaches a global minimum and diverges to $+\infty$ when $r \rightarrow 0$ as shown in figure 1. When they exist, the apoastron at distance r_a and periastron at r_p of a PRO are given by the two intersections of the graph of ψ_e with constant ξ -lines. For a given energy ξ_c corresponding to the minimum of ψ_e , the distance $r_a = r_p$ and the orbit is circular.

In order to clarify the vocabulary we will use, let us define two fundamental potentials in this context.

Definition 2.1. *The harmonic potential is defined by $\psi_{\text{ha}}(r) = \frac{1}{2}\omega^2 r^2$ with $\omega \neq 0$. We call the potential $\psi_{\text{ke}}(r) = -\frac{\mu}{r}$ with $\mu > 0$ a Keplerian potential.*

To get the existence of a global minimum of the effective potential ψ_e and hence of PRO’s, we have to specify the behavior of the potential ψ when $r \rightarrow 0$. This is the objective of the following lemma.

¹This restriction characterizes the gravitational interaction for which Gauss’ theorem in spherical symmetry indicates that $\frac{d\psi}{dr} = \frac{GM(r)}{r^2} > 0$.

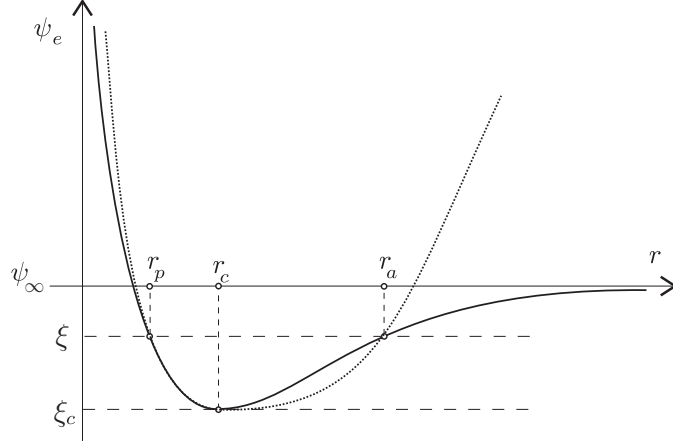


Figure 1: Physical effective potentials that allow Periodic Radial Orbits. The solid curve corresponds to a finite ψ_∞ and the dashed curve corresponds to an infinite ψ_∞ .

Lemma 2.1. *If for some $\Lambda \geq 0$, the effective potential $\psi_e(r) \rightarrow +\infty$ when $r \rightarrow 0$, then $\lim_{r \rightarrow 0} r^2 \psi(r) = \ell < \infty$. Conversely, if $\lim_{r \rightarrow 0} r^2 \psi(r) = \ell < \infty$, then for any $\Lambda \geq 0$ the effective potential $\psi_e(r) \rightarrow +\infty$ when $r \rightarrow 0$ provided that $\ell > -\Lambda^2$.*

Proof. The converse claim is obvious since $\lim_{r \rightarrow 0} r^2 \psi_e(r) = \Lambda^2 + \ell > 0$ if $\ell > -\Lambda^2$. For the first claim, let us assume that $\lim_{r \rightarrow 0} r^2 \psi(r)$ is infinite. Then $\lim_{r \rightarrow 0} \psi(r)$ is also infinite. But since $r \mapsto \psi(r)$ is increasing we must have $\lim_{r \rightarrow 0} \psi(r) = -\infty$. So for any $\Lambda > 0$, by choosing r close enough to 0, we would get

$$r^2 \psi(r) < -\Lambda^2 \implies \psi(r) < -\frac{\Lambda^2}{r^2} \implies \psi_e(r) < -\frac{\Lambda^2}{2r^2}$$

which implies $\lim_{r \rightarrow 0} \psi_e(r) = -\infty$. The claim follows by contraposition. \square

\square

These restrictions allow a PRO provided that $\xi \in [\xi_c, \psi_\infty)$, where $\psi_\infty = \lim_{r \rightarrow +\infty} \psi(r)$ may be infinite. The total and/or the central mass of such

systems could be infinite but the radial period

$$\tau_r = 2 \int_{r_p}^{r_a} \frac{dr}{\sqrt{2[\xi - \psi(r)] - \frac{\Lambda^2}{r^2}}} \quad (2)$$

is always finite. This period corresponds to the total duration of the transfer from r_a to r_p and back, and it is also related to the ξ -derivative of the radial action \mathcal{A}_r , which gives the radial pulsation (see for example [6] p. 221)

$$\Omega_r^{-1} = \frac{\tau_r}{2\pi} = \frac{\partial \mathcal{A}_r}{\partial \xi} \text{ with } \mathcal{A}_r = \frac{1}{\pi} \int_{r_p}^{r_a} \sqrt{2[\xi - \psi(r)] - \frac{\Lambda^2}{r^2}} dr. \quad (3)$$

This radial action also generates the increment of the azimuthal angle $\Delta\varphi$ during the transfer from r_a to r_p and back given by

$$\frac{\Delta\varphi}{2\pi} = n_\varphi = -\frac{\partial \mathcal{A}_r}{\partial \Lambda}. \quad (4)$$

Both τ_r and $\Delta\varphi$ are clearly two functions of the two variables ξ and Λ . In May 1958, Michel Hénon pointed out that two fundamental potentials, i.e. the Keplerian and harmonic ones, have τ_r which only depends on ξ . One year later, in a seminal article in French [20] (for an English translation see [5]), he found a family of physical potentials for which this property remains valid. We propose to complete this characterization of isochrony by an equivalent property on the azimuthal angle: $\Delta\varphi$ only depends on Λ , see theorem A.1 in appendix A. This family is known as Hénon's Isochrone. We propose now to follow his steps to recover his result and eventually extend it by exhibiting the whole set of possible isochrones.

Introducing Hénon's variables,

$$x = 2r^2 \quad \text{and} \quad Y(x) = x\psi\left(\sqrt{x/2}\right), \quad (5)$$

one can see that the corresponding x -values of the periastron and apoastron, namely x_a and x_p , are the roots of the equation $Y(x) = \xi x - \Lambda^2$. As it is detailed in figure 2, for a fixed value ξ of the energy, the set of all points $(P_{a,i}; P_{p,i})$ on the lines $y_i(x) = \xi x - \Lambda_i^2$ with corresponding abscissa $x_{a,i}$ and $x_{p,i}$ form the graph of Y . Using a clever analysis Michel Hénon shows that τ_r only depends on ξ if and only if $P_0 I$ is proportional to $(x_{p,1} - x_{a,1})^2$ when Λ^2 is varying. After a much more involved analysis Hénon was able to prove that this property characterizes parabolas. This original proof is very technical and we give a new version of it in theorem B.1 of appendix B highlighting the analytical property of the potentials.

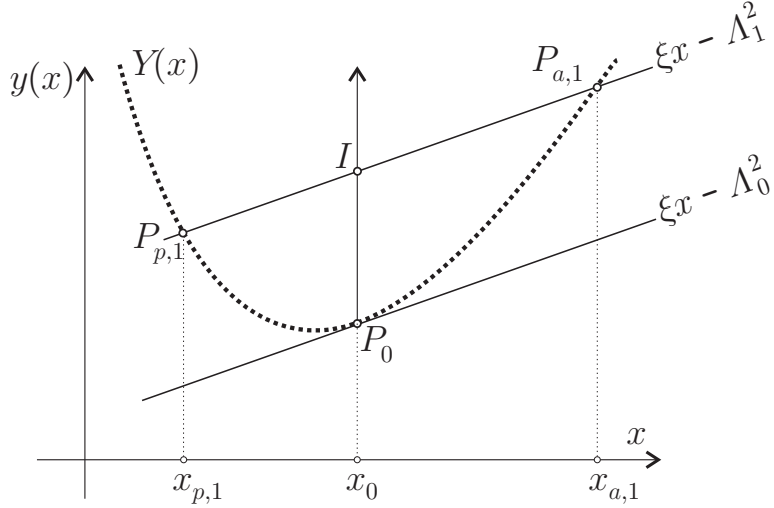


Figure 2: Geometric view of Hénon's variables.

2.2 General properties of isochrone parabolas

The general equation for a parabola in Hénon's variables is written as

$$(ax + bY)^2 + cx + dY + e = 0. \quad (6)$$

The expressions of the constants a , b , c , d and e in terms of the problem parameters are given in the original Hénon paper [20], where a and b cannot simultaneously vanish. From now on, the function defined by $\psi : x \mapsto Y(x)/x$ represents an isochrone potential according to the previous result. Two remarks allow us to simplify the parabola equation. First, any potential is defined up to a constant ϵ which enables us to map $\psi \rightarrow \psi + \epsilon$ or $Y \rightarrow Y + \epsilon x$ without loss of generality. This transformation is named an ϵ -*transvection* $(x, Y) \rightarrow (x, Y + \epsilon x)$. Second, by inspection of equation (1), one can see that if ψ is isochrone then the potential $\psi^*(r) = \psi(r) + j_\lambda(r)$ where $j_\lambda(r) = \frac{\lambda}{2r^2}$ is also isochrone with a new value of the angular momentum $\Lambda'^2 = \Lambda^2 + \lambda > 0$. In terms of Y this allows the transformation $Y \rightarrow Y^* = Y + \lambda$. Let us call this translation of the parabola a λ -*gauge* transformation of an isochrone potential. The action of a λ -gauge or ϵ -transvection could be synthesized in an affine transformation which is denoted as

$$J_{\epsilon, \lambda} : \begin{array}{ccc} \mathbb{R}^2 & \rightarrow & \mathbb{R}^2 \\ (x, Y) & \mapsto & (x, Y + \epsilon x + \lambda). \end{array}$$

If we denote by \mathbb{A} the set of these affine transformations $J_{\epsilon,\lambda}$ and by observing that $J_{\epsilon,\lambda} \circ J_{\epsilon',\lambda'} = J_{\epsilon+\epsilon',\lambda+\lambda'}$, we see that it is a subgroup of affine transformations of the real plane, isomorphic to $(\mathbb{R}^2, +)$. Affine transformations in Hénon's variables correspond to physical transformations which preserve the isochrone property. From this, we arrive at three short lemmas to organize the discussion.

Lemma 2.2. *With a vertical translation $J_{0,\lambda} : Y \rightarrow Y^* = Y + \lambda$, the Hénon Parabola can be reduced to a non-degenerate parabola passing through the origin of the (x, y) -axis.*

Proof. According to lemma 2.1, $\ell = \lim_{r \rightarrow 0} r^2 \psi(r)$ is a real number. By plugging the potential in equation (6) with the Hénon change of variables, we get

$$[2ar^2 + 2br^2\psi(r)]^2 + 2cr^2 + 2dr^2\psi(r) + e = 0.$$

Taking the limit as $r \rightarrow 0$ we get

$$4b^2\ell^2 + 2d\ell + e = 0. \quad (7)$$

Now, the λ -translation $Y \rightarrow Y^* = Y + \lambda$ changes the potential to $\psi^*(r) = \psi(r) + \frac{\lambda}{2r^2}$ and hence $\ell^* = \lim_{r \rightarrow 0} r^2 \psi^*(r) = \ell + \frac{\lambda}{2}$. So by taking $\lambda = -2\ell$ we have $\ell^* = 0$. Therefore, according to (7), we have $e^* = 0$ for the new parabola. In other words, the translated parabola passes through the origin of the (x, y) -axis. The degenerate cases of parabolas, where a/b (resp. b/a) is proportional to c/d (resp. d/c) or $d = c = 0$ or $a = b = 0$, are not of interest in our study since they lead to constant potentials up to a gauge. \square

Considering the result of lemma 2.2, it is now possible to consider the asymptotic behavior of the isochrone potential ψ associated with Y , which is given by the relation

$$(A + B\psi)^2 = \frac{C\psi + D}{2r^2}. \quad (8)$$

Let $\mathcal{D}_\psi \subset \mathbb{R}^+$ be the domain on which the potential is defined physically. Then, let us introduce

$$\mathcal{R} = \sup_{\mathbb{R}} [\mathcal{D}_\psi], \quad (9)$$

where a priori \mathcal{R} is finite and positive if \mathcal{D}_ψ is bounded or $\mathcal{R} = +\infty$ if not. We additionally define $\psi_\infty = \lim_{r \rightarrow \mathcal{R}} \psi(r)$. We now have the following lemma:

Lemma 2.3. *In the context of the above reduction given by (8) we have the following equivalences: ψ_∞ is infinite if and only if $B = 0$ if and only if ψ is harmonic up to an additive constant.*

Proof. • If $B = 0$ then, according to lemma 2.2, $C \neq 0$ and from (8) we get $\psi(r) = 2\frac{A^2}{C}r^2 - \frac{D}{C}$. As we are only interested in increasing potentials, C is positive and $\psi(r) = \psi_{\text{ha}}(r) = \frac{1}{2}\omega^2 r^2$ with $\omega \neq 0$ — up to an additive constant. This potential is defined on $[0, +\infty)$ so $\mathcal{R} = +\infty$ and $\psi_\infty = +\infty$.

- Let us assume conversely that ψ_∞ is infinite. As the potential is increasing, there exists an r_0 in the neighborhood of \mathcal{R} such that for all $r > r_0$, $\psi(r) > 0$. By dividing equation (8) by ψ for $r > r_0$, we get

$$\frac{1}{\psi}(A + B\psi)^2 = \frac{1}{2r^2} \left(C + \frac{D}{\psi} \right).$$

The right hand side of this equality tends to the finite limit $\frac{C}{2\mathcal{R}^2}$ when $r \rightarrow \mathcal{R}$ (that is to zero if $\mathcal{R} = +\infty$). If $B \neq 0$, since $\psi_\infty = +\infty$, the left hand side tends to $+\infty$ when $r \rightarrow \mathcal{R}$. Therefore, ψ_∞ infinite implies that $B = 0$ and ψ is harmonic by the first part of this analysis. \square

\square

The quantity ψ_∞ indicates the asymptotic direction of the parabola. When $\psi_\infty = +\infty$, then the symmetry axis of the parabola is parallel to (Oy) . We do not consider the case $\psi_\infty = -\infty$ because it corresponds to bottom-oriented parabolas which are always associated with decreasing harmonic potentials $\psi_{\text{ha}}^-(r) = -\frac{1}{2}\omega^2 r^2$. In this case the effective potential never has global nor local minima and no orbit could ever be periodic.

Before exhibiting the isochrone potentials we can say a little more about the tangent to the parabola at the origin.

Lemma 2.4. *For a potential given by (8), two cases may happen concerning the tangent at the origin of the isochrone parabola:*

1. *It is vertical and the reduced potential is Keplerian up to an additive constant. This corresponds to $C = 0$ in (8).*
2. *It is not vertical and modulo a transvection we can manage to get a horizontal tangent corresponding to $D = 0$ in the transvected version of (8).*

Proof. With a gauge transformation we may write the isochrone parabola equation as $(Ax + BY)^2 = CY + Dx$. Let us apply to it a transvection with a parameter ϵ . The new equation is then

$$(A'x + B'Y)^2 = C'Y + D'x \quad \text{with} \quad \begin{cases} A' = A + B\epsilon, C' = C \\ B' = B \text{ and } D' = D + C\epsilon. \end{cases} \quad (10)$$

By considering the gradient of the function $f(x, y) = (A'x + B'y)^2 - C'y - D'x$ at the origin, we get the equation of the tangent to the parabola at the origin, $D'x + C'y = 0$. Depending on its direction, two cases may be distinguished:

1. When $C = 0$, the parabola passes through the origin with a vertical tangent. One may further simplify the parabolic equation choosing ϵ to cancel A' since B should be non-zero according to lemma 2.2. We eventually obtain $(B')^2Y^2 = D'x$. This equation implies that $D' > 0$. Making explicit Hénon variables with (5), we get $\psi(r) = \psi_{\text{ke}}(r) = -\frac{\mu}{r}$ where $\mu = \sqrt{\frac{D'}{2B'^2}}$ is a positive constant since $r \mapsto \psi(r)$ is increasing.
2. When $C \neq 0$, it is possible to choose the parameter ϵ of the transvection to cancel D' so that the parabola passes through the origin with a horizontal tangent. In other words, we choose the arbitrary constant of the potential to simplify the study of its corresponding parabola, which may be described by $(A'x + B'Y)^2 = C'Y$ with $A' \neq 0$. A' cannot vanish unless $\epsilon = -\frac{A}{B} = -\frac{D}{C}$ which is forbidden by lemma 2.2. □

□

Let us summarize the situation at this point (see figure 3).

Any parabola in the plane (x, y) is associated with an isochrone potential. Combining lemmas 2.2, 2.3 and 2.4 we can only study the family of parabolas passing through the origin and belonging to one of the two following classes:

- Straight parabolas, which possess a vertical symmetry axis and thus never admit any vertical tangent. As we have explained before we are only interested by straight up-oriented parabolas. Using affine transformations, straight parabolas could be moved in such a manner that their apices are the origin of the (x, y) -plane. They correspond to harmonic potentials.

- Tilted parabolas, whose symmetry axes are inclined from the vertical ones and possess a horizontal or vertical tangent at the origin. This tilted parabola family is composed of three categories:
 - Laid parabolas, with a vertical tangent at the origin corresponding to Kepler potentials;
 - Right-oriented parabolas, with a horizontal tangent at the origin;
 - Left-oriented parabolas, with a horizontal tangent at the origin.

In figure 3, we have plotted in the (xOy) plane the four *reduced* classes of parabolas. A precise definition of the corresponding potentials is given in definition 2.2 p.19.

The reduced isochrone potential contained in each reduced parabola is emphasized in this figure and it corresponds to a limited part of the parabola. As a matter of fact, the variable of the potential is the radial distance, a positive real number. Each isochrone potential is then included in the x -positive right plane. This remark excludes left-oriented laid parabolas. For any non-straight parabolas there are two functions $x \mapsto y_1(x)$ and $x \mapsto y_2(x)$ into which the x -positive part of the graph of the parabola could be decomposed (see figure 3). The slope of the chord between the origin and a point M of abscissa $x > 0$ on the graph of y_1 or y_2 is given by the ratio $\frac{y_1(x)}{x}$ or $\frac{y_2(x)}{x}$ which is precisely the definition of the potential ψ . This remark shows that ψ is an increasing (resp. decreasing) function if the graph of y is convex (resp. concave), i.e. the chord between two points is above (resp. below) the function. As we look for increasing potentials in order to have PRO's, we have to consider the convex part of the parabola graph. This part is named y_1 in figure 3.

Tilted parabolas have a symmetry axis with a finite slope. Any ϵ -transvection adds ϵ to this slope, modifying the orientation of these parabolas. Nevertheless, we cannot jump from a left-oriented parabola to a right-oriented one using an affine transformation. However, according to lemma 2.4 and conserving its orientation, we can morph any tilted parabola with a horizontal tangent or a vertical tangent at the origin. In the latter case, the symmetry axis is parallel to (Ox) . The morphing from the reduced parabolas to the whole set of isochrone ones is detailed in figure 5 following our analysis of the concerned potentials in the next section.

Our reduction to four families of parabolas and their corresponding potentials enables us to obtain the whole set of isochrone potentials. In his historical study, Michel Hénon did not remark on the crucial role of these

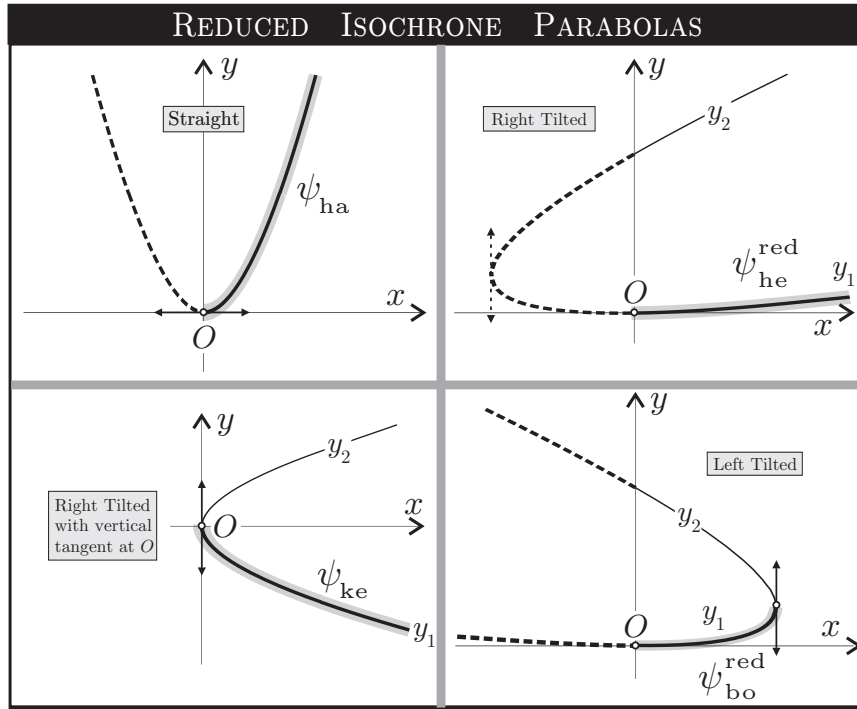


Figure 3: The four classes of reduced parabolas corresponding to the reduced isochrone potentials. The part of the parabola associated with the increasing potential is highlighted (y_1). The dashed part of the parabola corresponds to potentials with an imaginary distance argument ($x < 0$). The unhighlighted solid line part of the parabola (y_2) in the $x > 0$ half-plane corresponds to decreasing potentials.

affine transformations. He dismissed out-of-origin parabolas and forgot left-oriented tilted ones.

Let us now determine explicitly the isochrone potentials of the reduced families.

2.3 Classification of isochrone potentials

From the previous analysis we will now state and prove the following classification result.

Theorem 2.5. *The isochrone potentials are classified by these two properties:*

1. *There are essentially four types of reduced isochrone potentials:*
 - *The Keplerian potential ψ_{ke} for which the reduced parabola has a horizontal symmetry axis and a vertical tangent at the origin.*
 - *The harmonic potential ψ_{ha} for which the reduced parabola is straight with a horizontal tangent at the origin.*
 - *Two other potentials $\psi_{\text{he}}^{\text{red}}$ and $\psi_{\text{bo}}^{\text{red}}$ for which the reduced parabolas have horizontal tangents at the origin and are respectively right and left oriented. They are given by the formulae*

$$\psi_{\text{he}}^{\text{red}} := \frac{\mu}{2b} - \frac{\mu}{b + \sqrt{b^2 + r^2}}, \quad \psi_{\text{bo}}^{\text{red}} := -\frac{\mu}{2b} + \frac{\mu}{b + \sqrt{b^2 - r^2}},$$

where μ and b are positive constants.

2. *Any isochrone potential ψ is equivalent under an affine transformation to one of the previous types. That is to say there exist two constants ϵ and λ and some reduced potential $\psi^{\text{red}} \in \{\psi_{\text{ke}}, \psi_{\text{ha}}, \psi_{\text{he}}^{\text{red}}, \psi_{\text{bo}}^{\text{red}}\}$ such that $\psi(r) = \psi^{\text{red}}(r) + \epsilon + \frac{\lambda}{2r^2}$.*

The potential ψ_{he} is the original potential discovered by Michel Hénon. From our knowledge, the potential ψ_{bo} is a new one. We call it the *bounded* potential for reasons appearing in sec. 2.4.

Proof. Let \mathcal{P} be the parabola associated with an isochrone potential ψ which is neither Keplerian nor harmonic. According to lemmas 2.2, 2.3 and 2.4 we are left to consider the case where \mathcal{P} passes through the origin, has a horizontal tangent and has a symmetry axis which is not vertical. According

to (8) and the previous lemmas, this corresponds to having an equation of the form

$$2r^2 = \frac{n\psi}{(\psi - m)^2},$$

for some constant m and n both non zero. As a consequence, we see here that the potential ψ will depend on two constants. Normalizing the potential by setting $\psi = mV$, we are led to the functional equation

$$q = q(V) = \frac{V}{(V - 1)^2}, \quad \text{with} \quad q = \kappa x = 2\kappa r^2,$$

where $\kappa = m/n$ is another non zero constant. The inversion of the function q gives two solutions $V(q)$ of the quadratic equation

$$qV^2 - (2q + 1)V + q = 0. \quad (11)$$

They are of the form

$$\begin{cases} V^+(q) & := \frac{2q+1-\sqrt{4q+1}}{2q} = 1 - \frac{2}{1+\sqrt{4q+1}}, \\ V^-(q) & := \frac{2q+1+\sqrt{4q+1}}{2q} = 1 - \frac{2}{1-\sqrt{4q+1}}. \end{cases} \quad (12)$$

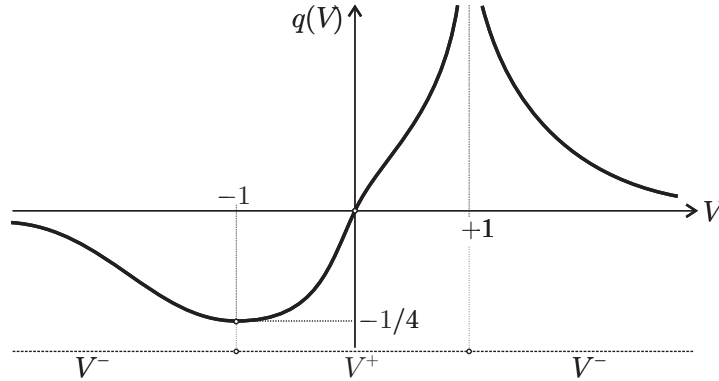


Figure 4: The potential V^+ and V^- as functions of q .

These two functions $q \mapsto V(q)$ are defined on the real interval $q \geq -1/4$. As shown in figure 4, the \pm signs of V are chosen in such a way that $q \mapsto V^+(q)$ is increasing on $[-1/4, +\infty)$ and $q \mapsto V^-(q)$ is decreasing on both $[-1/4, 0)$ and $]0, +\infty)$. From the quadratic equation (11) we have

$$V^+(q) + V^-(q) = 2 + \frac{1}{q} \quad \text{and} \quad V^+(q)V^-(q) = 1. \quad (13)$$

Now we compute the potential. From the expression $q = \kappa x = 2\kappa r^2$, we will classify the potentials by the sign of the constant κ .

1. **When $\kappa < \mathbf{0}$** , then q is necessarily negative. Therefore $-1/4 \leq q \leq 0$ which implies

$$r^2 \leq \frac{1}{8|\kappa|}.$$

Setting a new constant $b := \frac{1}{\sqrt{8|\kappa|}}$ in such a way that the previous inequality becomes $r \leq b$, we have $q = \frac{-r^2}{4b^2}$. Therefore,

$$\psi(r) = mV(q) = mV\left(\frac{-r^2}{4b^2}\right).$$

This gives us two possible potentials ψ^\pm . But to have a PRO, the function $r \mapsto \psi(r)$ must be ultimately increasing. That is,

$$\frac{-mr}{2b^2} \frac{dV}{dq}\left(\frac{-r^2}{4b^2}\right) > 0.$$

Since $q \mapsto V^+(q)$ is increasing we must choose $m = -\frac{\mu}{2b}$ for some positive constant μ . The factor $\frac{1}{2b}$ is just here for simplicity of the final result. Similarly in the formula for ψ^- we must choose $m = \frac{\mu}{2b} > 0$. This leads to the two potentials

$$\begin{cases} \psi_{\text{bo}}^+(r) & := -\frac{\mu}{2b} V^+\left(\frac{-r^2}{4b^2}\right) & = -\frac{\mu}{2b} + \frac{\mu}{b+\sqrt{b^2-r^2}}, \\ \psi_{\text{bo}}^-(r) & := \frac{\mu}{2b} V^-\left(\frac{-r^2}{4b^2}\right) & = \frac{\mu}{2b} - \frac{\mu}{b-\sqrt{b^2-r^2}}. \end{cases}$$

From (13), we get that

$$\psi_{\text{bo}}^-(r) - \psi_{\text{bo}}^+(r) = \frac{\mu}{2b} \left[V^+\left(\frac{-r^2}{4b^2}\right) + V^-\left(\frac{-r^2}{4b^2}\right) \right] = \frac{\mu}{b} - \frac{2b\mu}{r^2}. \quad (14)$$

As a consequence, the left-oriented parabolas associated with ψ_{bo}^+ and ψ_{bo}^- are exchanged by an affine transformation. This is the meaning of the word *essentially* in the statement of the theorem since the group orbits of $\psi_{\text{bo}}^{\text{red}} := \psi_{\text{bo}}^+$ and of ψ_{bo}^- under the action of the affine group are the same.

2. **When $\kappa > \mathbf{0}$** , setting $b := 1/\sqrt{8\kappa}$ again, we similarly get $\psi = mV(q) = mV\left(\frac{r^2}{4b^2}\right)$. And by setting again $\frac{\mu}{2b} := |m|$ we get two new isochrone potentials

$$\begin{cases} \psi_{\text{he}}^+(r) & := \frac{\mu}{2b} V^+\left(\frac{r^2}{4b^2}\right) & = \frac{\mu}{2b} - \frac{\mu}{b+\sqrt{b^2+r^2}}, \\ \psi_{\text{he}}^-(r) & := -\frac{\mu}{2b} V^-\left(\frac{r^2}{4b^2}\right) & = -\frac{\mu}{2b} + \frac{\mu}{b-\sqrt{b^2+r^2}}. \end{cases}$$

Again from (13), we have that

$$\psi_{\text{he}}^+(r) - \psi_{\text{he}}^-(r) = \frac{\mu}{2b} \left[V^+ \left(\frac{r^2}{4b^2} \right) + V^- \left(\frac{r^2}{4b^2} \right) \right] = \frac{\mu}{b} + \frac{2b\mu}{r^2}. \quad (15)$$

Therefore, $\psi_{\text{he}}^{\text{red}} := \psi_{\text{he}}^+$ and ψ_{he}^- are also exchanged by the affine group and their respective group orbits under this group action will coincide. These potentials are defined for all values of $r \in [0, +\infty)$ so that their parabolas are then right-oriented.

To conclude the proof of the theorem we only have to observe that according to lemmas 2.2, 2.3 and 2.4, any isochrone is in the orbit of a reduced one under the affine subgroup generated by the $J_{\epsilon, \lambda}$ transformations. \square \square

These reduced potentials can be visualized in figure 3.

Using natural notations taken from the proof of theorem 2.5, from (14) and (15) we can write

$$\begin{cases} \psi_{\text{bo}}^- = J_{+\epsilon, \lambda}(\psi_{\text{bo}}^+) \\ \psi_{\text{he}}^- = J_{-\epsilon, \lambda}(\psi_{\text{he}}^+) \end{cases} \quad \text{with } \epsilon = \frac{\mu}{b} \text{ and } \lambda = -4b\mu. \quad (16)$$

The tilted parabolas presented in figure 3 are the ones associated with ψ_{he}^+ for the right (called $\mathcal{P}_{\text{he}}^+$) parabola and with ψ_{bo}^+ for the left one (called $\mathcal{P}_{\text{bo}}^+$). These two parabolas both open to the top, i.e. in the direction where y increases. Using property (16) or by direct representation, one can verify that, using natural notations, $\mathcal{P}_{\text{he}}^-$ (resp. $\mathcal{P}_{\text{bo}}^-$) is the image of $\mathcal{P}_{\text{he}}^+$ (resp. $\mathcal{P}_{\text{bo}}^+$) by the symmetry under the (O, x) -axis. Thus, these two “negative” parabolas both open to the bottom.

2.4 Some physical meaning of this classification

The potential $\psi_{\text{he}}^{\text{red}}$ defined by

$$\psi_{\text{he}}^{\text{red}}(r) := \frac{\mu}{2b} - \frac{\mu}{b + \sqrt{b^2 + r^2}}$$

is the original isochrone potential discovered by Michel Hénon. Similarly, the potential

$$\psi_{\text{bo}}^{\text{red}} := -\frac{\mu}{2b} + \frac{\mu}{b + \sqrt{b^2 - r^2}}$$

defines another type of isochrone potential. The index *bo* means *bounded potential*. Indeed, from the above formula the mappings $r \mapsto \psi_{\text{bo}}^{\text{red}}(r) + \epsilon$ are only defined for bounded values of

$$r \in \mathcal{D}_{\psi_{\text{bo}}} = [0, b]. \quad (17)$$

The fact that such potentials are associated with a *bounded* system give them special features which are very different from the three other types of isochrone potentials. Up to our knowledge, such bounded potentials do not seem to have appeared in the literature before.

The potential of Michel Hénon is equivalent to a Keplerian one when $r \rightarrow \infty$. Using relation (12), we can readily see that $V^+(q) \sim q$ when $q \rightarrow 0$. The roots product in (13) then implies $V^-(q) \sim q^{-1}$ in the same limit. Then both $\psi_{\text{bo}}^{\text{red}}$ and $\psi_{\text{he}}^{\text{red}}$ come from V^+ . Hence we can assert that they are harmonic near their center: $\psi_{\text{bo}}^{\text{red}} \sim \psi_{\text{he}}^{\text{red}} \sim \psi_{\text{ha}}$ when $r \rightarrow 0$.

From a physical point of view, ϵ -transvections $J_{\epsilon,0} : \psi \rightarrow \psi + \epsilon$ add a constant to the potential, hence they do not change anything for the dynamics in the considered potential, changing only the value of the energy attributed to the trajectories.

When the λ -gauge $J_{0,\lambda} : \psi \rightarrow \psi + \frac{\lambda}{2r^2}$ is applied to a reduced potential, it makes it divergent as r^{-2} when $r \rightarrow 0$. As we said at the beginning of sec. 2.2, such transformations correspond to a change of the value of the angular momentum in the corresponding isochrone orbit.

Geometrically, when the physical convex part of the parabola starts from the origin, then, when $r \rightarrow 0$, the corresponding potential is finite (if it is ψ_{bo} , ψ_{he} or ψ_{ha}) or diverges like r^{-1} (if it is Keplerian). This behavior is not perturbed by ϵ -transvections. In all other cases isochrone potentials diverge like r^{-2} when $r \rightarrow 0$; but, using a λ -translation, we can manage this physical problem.

These remarks enable us to define three classes of isochrone potentials. They are classes of equivalence under the action of $J_{\epsilon,\lambda}$ affine transformations as detailed in sec. 2.5. Definition 2.2 sets their names in addition to the name of the four isochrone potential types.

Definition 2.2. 1. We call the four isochrone potentials

$$\begin{aligned} \psi_{\text{ke}}(r) &= -\frac{\mu}{r}, & \psi_{\text{ha}}(r) &= \frac{1}{2}\omega^2 r^2, \\ \psi_{\text{he}}(r) &= -\frac{\mu}{b + \sqrt{b^2 + r^2}}, & \text{and } \psi_{\text{bo}}(r) &= \frac{\mu}{b + \sqrt{b^2 - r^2}}, \end{aligned}$$

the Kepler, the harmonic, the Hénon and the bounded potential, respectively.

2. We call reduced isochrone potentials $\psi_{\text{iso}}^{\text{red}}$ one of the four potentials

$$\psi_{\text{ke}}, \psi_{\text{ha}}, \psi_{\text{he}}^{\text{red}} = J_{\frac{\mu}{2b}, 0}(\psi_{\text{he}}) = \frac{\mu}{2b} + \psi_{\text{he}} \text{ or } \psi_{\text{bo}}^{\text{red}} = J_{-\frac{\mu}{2b}, 0}(\psi_{\text{bo}}) = -\frac{\mu}{2b} + \psi_{\text{bo}}.$$

3. We call physical isochrone potentials $\psi_{\text{iso}}^{\text{phy}}$ the result of a transvection applied to a reduced isochrone: $\psi_{\text{iso}}^{\text{phy}} = J_{\epsilon, 0}(\psi_{\text{iso}}^{\text{red}}) = \psi_{\text{iso}}^{\text{red}} + \epsilon$.

4. We call gauged isochrone potentials $\psi_{\text{iso}}^{\text{gau}}$ the result of a vertical translation applied to a physical isochrone: $\psi_{\text{iso}}^{\text{gau}} = J_{0, \lambda}(\psi_{\text{iso}}^{\text{phys}}) = \psi_{\text{iso}}^{\text{phys}} + \frac{\lambda}{2r^2}$.

Physical isochrones possess interesting physical properties which are presented and studied in section 4. They all confine a finite mass in a finite radius $r < \mathcal{R}$ (see equation (9), page 10). Reduced isochrones are special cases of physical ones: their parabolas pass through the origin with a horizontal or a vertical tangent.

Due to their r^{-2} divergence in the potential, when $\lambda \neq 0$, gauged isochrone potentials have an infinite mass at their center and thus possess poor physical meaning. However, they are essential to the completeness of the isochrone set.

2.5 The affine group action on the Isochrone set

Let us denote respectively \mathbb{I}_{pot} and \mathbb{I}_{par} the set of isochrone potentials and parabolas. These two sets are in bijection and theorem 2.5 states that, from a mathematical point of view, they are four-dimensional manifolds. As a matter of fact, each isochrone potential is uniquely determined by four real parameters $(\mu, b, \epsilon, \lambda)$ with $\mu > 0$, $b \geq 0$ and $(\epsilon, \lambda) \in \mathbb{R}^2$ — n.b. for ψ_{bo} , $b > 0$.

We have also seen that the two-dimensional affine group $\mathbb{A} \simeq (\mathbb{R}^2, +)$, generated by the affine transformations $J_{\epsilon, \lambda}$ with $(\epsilon, \lambda) \in \mathbb{R}^2$, acts on both sets, either on potentials or on the corresponding parabolas. Since the dimension of \mathbb{A} is less than the dimension of \mathbb{I}_{pot} and \mathbb{I}_{par} ($2 < 4$), the action is not transitive and each group orbit $\mathbb{A} \cdot \psi$ or $\mathbb{A} \cdot \mathcal{P}$ for corresponding potential ψ or parabola \mathcal{P} is a two-dimensional sub-manifold of \mathbb{I}_{pot} or \mathbb{I}_{par} . This translates the second part of theorem 2.5: we have four types of group

orbits under the action of \mathbb{A} , one for each type of isochrone potential.

Let us now see more precisely this action of the affine group and its corresponding group orbits.

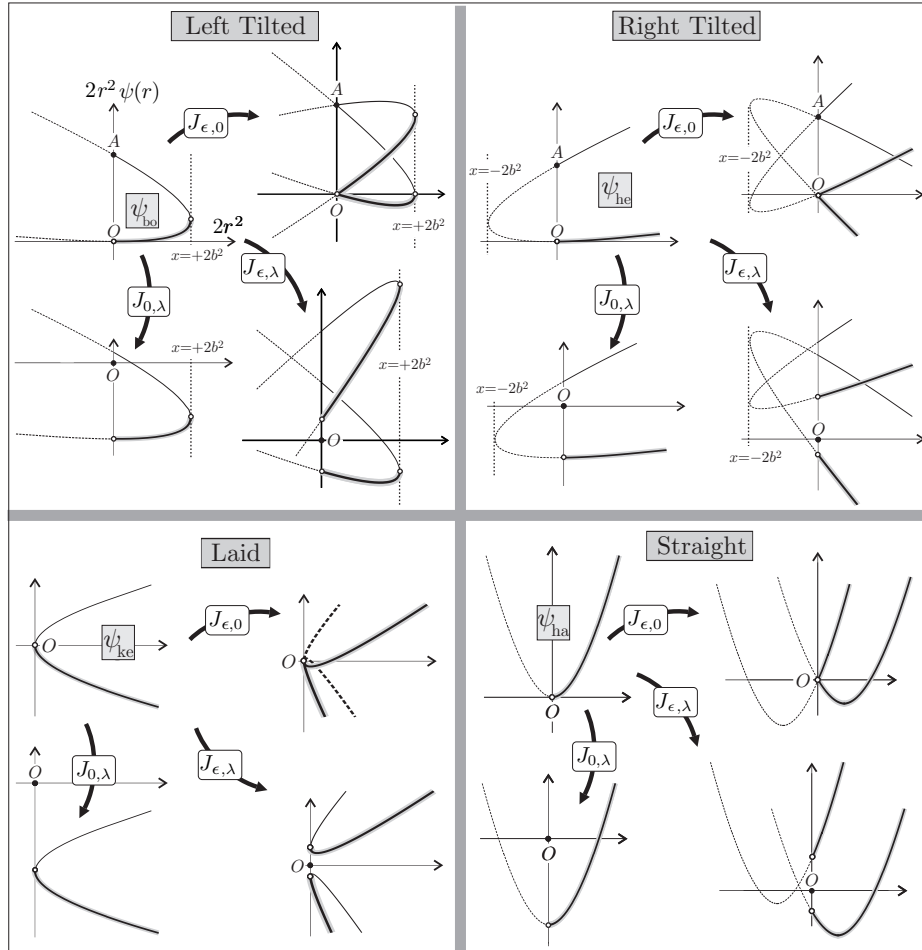


Figure 5: The action of affine transformations on reduced parabolas and their corresponding potentials.

Each parabola is associated with an isochrone potential and vice-versa. Each isochrone parabola belongs to one of the four classes of reduced parabolas we have presented in figure 3 and is associated with one of the four reduced isochrone potentials made explicit in theorem 2.5. In order to geometrically understand the morphing of parabolas associated with the

action of affine transformations, we propose the general picture of figure 5.

We do not represent in this figure either the bottom-oriented straight parabolas or the left-oriented laid ones because they respectively correspond to decreasing and non-physical potentials. We specify that it is always possible to have (Oy) -axis crossing the parabola: this corresponds to a horizontal translation of the parabola associated with a good choice of the origin of the physical referential.

Transvections correspond to $J_{\epsilon,0}$. They are associated with a swivel combined with a deformation of the parabola: the points of the parabola lying on the (Oy) -axis are invariant as is the abscissa of the vertical tangent.

General affine transformations $J_{\epsilon,\lambda}$ swivel, deform and translate a reduced parabola. They affect both the energy and the angular momentum of the considered isochrone orbit. Any parabola obtained from the action of $J_{\epsilon,\lambda}$ on a reduced one corresponds to an isochrone potential in the same group orbit of the reduced potential under the action of the Affine Group. In this sense we can claim that there are only four different isochrone potentials up to an affinity on its parabola.

We note that relations exist between the isochrone potentials. As a matter of fact, ψ_{ke} and ψ_{ha} come from ψ_{he} when $b \rightarrow 0$ and $b \rightarrow +\infty$, respectively. Furthermore, known relations exist between ψ_{ke} and ψ_{ha} , such as the Bohlin transformation ([7], [3], [31], see also the footnote 3 p.26) which maps the harmonic orbits onto Keplerian ones and vice versa. All these relations are not in the scope of the affine group action and do not affect the parameters (μ, b) or ω of the concerned potentials.

Nevertheless, making use of rotations R_θ of an angle θ in the (x, y) -frame and starting, for instance, from the laid Kepler parabola, we can obtain a new parabola with an arbitrarily oriented axis of symmetry. Then, acting with $J_{\epsilon,\lambda}$, we can recover the corresponding reduced parabola in one of the four families. This operation is graphically illustrated in figure 6 in the case of the morphing from the Kepler isochrone to the Hénon isochrone.

Varying the unique parameter μ of the Kepler potential, written as

$$y_{\text{ke}}(x) = -\mu\sqrt{2x} \tag{18}$$

in Hénon's variables, the aperture of its laid parabola varies and produces a variation of the b parameter of the Hénon potential corresponding to the negative part of the rotated parabola. Using this process one can easily understand that when $\theta \in (-\frac{\pi}{2}, +\frac{\pi}{2})$, we recover a Hénon potential ψ_{he} ; when $\theta \in (\frac{\pi}{2}, +\frac{3\pi}{2})$, we recover the bounded potential ψ_{bo} ; and for $\theta = +\frac{\pi}{2}$,

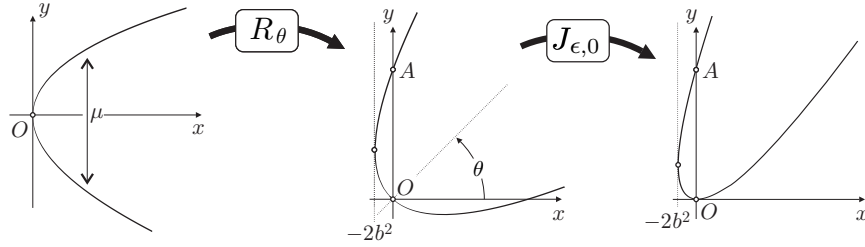


Figure 6: Rotation and transvection of the Kepler parabola to the Hénon one.

we obtain the harmonic ψ_{ha} from the Kepler potential ψ_{ke} . More generally, any isochrone potential is contained in the group orbit of a Kepler potential under the action of the group $\text{SO}(2) \times \mathbb{A}$.

As we have completely classified \mathbb{I}_{pot} and \mathbb{I}_{par} , we can now return to the study of isochrone PRO's. We will see that relevant isochrone rotations are not Euclidian but hyperbolic.

3 Isochrone orbits and isochrone transformations

3.1 Introduction and motivation

From the geometrical classification of the isochrone potentials established through the action of the Affine Group in section 2, we propose now to investigate isochrone orbits².

For this purpose, we generalize a transformation that originates in the work of Newton, Karl Bohlin [7] and Donald Lynden-Bell [30] who recently passed away and to whom we dedicate this work. He explored a remarkable property of Michel Hénon's isochrone, namely ψ_{he} is equivalent to a harmonic potential at small distances and to a Keplerian potential at larger ones, see section 4. In those two potentials, the orbits are closed ellipses. Newton showed, in the later edition of the Principia, how to map a Keplerian elliptical orbit onto a harmonic one and vice versa. His methods relied on a total exchange of energy and potential between a Kepler and a Hooke system. Pointing out a freedom that involves partial exchange of energy and potential, Donald Lynden-Bell derived Hénon's isochrone as a

²When not specified, orbit refers to the trajectory of the considered test particle in the considered potential and no more to the group orbit of a potential or parabola under a group action.

convex interpolation of Kepler and Hooke potentials. Let us detail now their mathematical analysis and generalize it to isochrone orbits transformations.

3.1.1 Isochrone orbits transformations

A Periodic Radial Orbit (PRO) $r_0(t_0)$ in a radial potential ψ_0 is governed by the ordinary differential equation

$$\frac{1}{2} \left(\frac{dr_0}{dt_0} \right)^2 + \frac{\Lambda_0^2}{2r_0^2} = \xi_0 - \psi_0(r_0).$$

In Hénon variables $x_0 = 2r_0^2$ and $y_0 = x_0\psi_0(x_0)$, it can be written as

$$\frac{1}{16} \left(\frac{dx_0}{dt_0} \right)^2 + \Lambda_0^2 = x_0\xi_0 - y_0(x_0). \quad (19)$$

Since the force derived from a radial potential is radial, the motion of a test particle takes place in a fixed plane and this particle is described by its polar coordinates (r_0, φ_0) in this plane.

When the potential is isochrone, y_0 is a parabola. This property is preserved by linear transformations of parabolas (see lemma C.1 in appendix C) and consequently for the orbits they contain. Placing the origin of the (x, y) -plane at the center of the system described by ψ_0 , linear transformations relate isochrone orbits together. There exists then a change of variables $(r_0, t_0) \mapsto (r_1, t_1)$ mapping an isochrone orbit onto another one that satisfies an orbital equation in the new potential y_1 , i.e.

$$\frac{1}{16} \left(\frac{dx_1}{dt_1} \right)^2 + \Lambda_1^2 = x_1\xi_1 - y_1(x_1). \quad (20)$$

As Donald Lynden-Bell explained ([31] sect. 3 or [30] sect. 2), it is convenient to study orbits of identical angular momentum

$$\Lambda_1 = \Lambda_0 = \Lambda. \quad (21)$$

This hypothesis allows one to get the same Kepler's area law for both orbits, in their respective radial potentials.

At this point, no constraints specify how each of the three remaining terms $\left(\frac{dx_0}{dt_0} \right)^2$, $x_0\xi_0$, and y_0 in (19) is transformed in the mapping. For instance, the Bohlin transformation (see [7] for the original reference or [3] for a modern presentation) consists of a full exchange between energy and

potential terms. As underlined by Lynden-Bell, the exchange can also be partial: only part of the potential term y_0 is then mapped onto the energy ξ_1 and vice versa. We thus propose to conserve

$$x_1\xi_1 - y_1(x_1) = x_0\xi_0 - y_0(x_0). \quad (22)$$

The two conditions (21) and (22) imply

$$\frac{dx_1}{dt_1} = \frac{dx_0}{dt_0} \quad \text{and} \quad 2\Lambda = x_0 \frac{d\varphi_0}{dt_0} = x_1 \frac{d\varphi_1}{dt_1} \quad (23)$$

for the radial and angular velocities of the orbits in the mapping.

The more general linear transformation of $\vec{w} = (\xi x, y)^\top$ satisfying the constraint (22) is given by

$$\vec{w}_1 = B_{\alpha,\beta}(\vec{w}_0) \quad \text{with} \quad B_{\alpha,\beta} = \begin{bmatrix} \alpha & \beta \\ \alpha - 1 & \beta + 1 \end{bmatrix}, \quad (\alpha, \beta) \in \mathbb{R}^2. \quad (24)$$

Lynden-Bell transformation only depends on one parameter with $\beta = 1 - \alpha$. From now on, we will assume $\det(B_{\alpha,\beta}) = \alpha + \beta \neq 0$ because the corresponding singular transformation leads to constant potentials or not well-defined image orbits. As a consequence, $B_{\alpha,\beta}$ will be invertible and can be used to change the reference frame. In this case we call $B_{\alpha,\beta}$ a *bolst* in the general case or an *ibolst* when it is symmetric. Reasons for these names will become clear later.

3.1.2 The bolst as the generalized Bohlin transformation

A bolst $B_{\alpha,\beta}$ maps two orbits in two isochrone potentials. It induces a change of time which can be made explicit: using (23) and (24) we get

$$\frac{dt_1}{dt_0} = \frac{dx_1}{dx_0} = \frac{\alpha\xi_0}{\xi_1} + \frac{\beta}{\xi_1} \frac{dy_0}{dx_0}. \quad (25)$$

We assume $\xi_1 \neq 0$ since associated orbits are not well-defined in the coordinates of \vec{w} . To deal with $\xi_1 = 0$ one may apply first a transvection $J_{\epsilon,0}$ to \vec{w} , then study the orbit with $\xi_1 + \epsilon \neq 0$.

In order to ensure a bijective time transformation $t_0 \rightarrow t_1(t_0)$, we need to impose a fixed sign on $\frac{dt_1}{dt_0}$. For instance, we assume it to be positive. Combining its expression (25) with the second condition of (23), the time evolution can be expressed in terms of the polar angles of the two orbits in their respective planes of motion. They are linked through

$$\left[\frac{\alpha\xi_0}{\xi_1} + \frac{\beta}{\xi_1} \frac{y_0}{x_0} \right] \frac{d\varphi_1}{d\varphi_0} = \frac{\alpha\xi_0}{\xi_1} + \frac{\beta}{\xi_1} \frac{dy_0}{dx_0} > 0. \quad (26)$$

As we will see below, this ODE gives φ_1 as a function of φ_0 , i.e. $\varphi_1(\varphi_0)$, when $y_0(x_0)$ is specified. When it is solved, the orbit can be plotted in polar coordinates (x_1, φ_1) . In the next proposition we solve this equation when a bolst is applied to a Keplerian orbit. In theorem 3.1, we call system a potential - orbit couple.

Theorem 3.1. *Only the harmonic and Keplerian potentials can exchange their radial orbits with a linear change of polar angle. The transformation of a Kepler system into a scaled Kepler system is given by $B_{\alpha,0}$. On the other hand, $B_{0,\beta}$ maps a Kepler system onto a harmonic one by fully exchanging the energy and potential. This is the classical Bohlin transformation³.*

Otherwise, when $\alpha\beta \neq 0$, the image of a Keplerian PRO by $B_{\alpha,\beta}$ is an isochrone orbit. Its azimuthal angle is given by

$$\varphi_1(\varphi_0) = \frac{\varphi_0}{2} + \frac{\chi}{\sqrt{(1+\chi)^2 - e^2}} \arctan \left[\sqrt{\frac{1+\chi-e}{1+\chi+e}} \tan \left(\frac{\varphi_0}{2} \right) \right] \quad \text{with } \chi = \frac{p\alpha |\xi_0|}{\mu\beta}, \quad (27)$$

where p and e are respectively the semilatus rectum and excentricity of the primary Keplerian orbit. The expression holds when $\alpha \rightarrow 0$ and for the neutral bolst $B_{\alpha,0}$ when $\beta \rightarrow 0$. The precession $\Delta\varphi_1$ of the transformed polar angle during the transfer from the periastron to the apoastron and back is given by

$$\Delta\varphi_1 = \pi \left(1 + \frac{\chi}{\sqrt{(1+\chi)^2 - e^2}} \right).$$

Proof. Assume potential ψ_0 to be ψ_{ke} . If the primary orbit is a PRO, then the radial distance is known by

$$\frac{1}{r_0} = \frac{1 + e \cos \varphi_0}{p},$$

where p and e are respectively the semilatus rectum and the excentricity of the Keplerian elliptic orbit of energy $\xi_0 < 0$ that we consider. Moreover, from equation (18), we have $y_0(x_0) = -\mu\sqrt{2x_0}$. Hence,

$$\frac{y_0}{x_0} = \psi_0 = -\frac{\mu}{r_0} \quad \text{and} \quad \frac{dy_0}{dx_0} = -\frac{\mu}{\sqrt{2x_0}} = -\frac{\mu}{2r_0}.$$

In this case, the ODE (26) becomes

$$\left[\alpha\xi_0 - \frac{\mu\beta}{p} (1 + e \cos \varphi_0) \right] \frac{d\varphi_1}{d\varphi_0} = \alpha\xi_0 - \frac{\mu\beta}{2p} (1 + e \cos \varphi_0)$$

³This transformation is also known as the transformation of Levi-Civita [27] and was already introduced by C. MacLaurin in [32] and then E. Goursat in [17] as excellently remarked by Alain Albouy and Niccolò Guicciardini.

for $\xi_1 \neq 0$. Two cases appear to be trivial:

1. When $\alpha = 0$ and $\beta \neq 0$, then

$$\frac{d\varphi_1}{d\varphi_0} = \frac{1}{2}.$$

The system (24) can be directly inverted and gives

$$\begin{cases} r_1^2 = -\frac{\beta\mu}{\xi_1}r_0, \\ \psi_1(r_1) = \beta_1 + \frac{1}{2}\omega_1 r_1^2, \end{cases} \quad \text{where } \omega_1^2 = \frac{2|\xi_0|\xi_1^2}{\mu^2\beta^2} \text{ and } \beta_1 = \frac{\beta+1}{\beta}\xi_1.$$

This duality between the harmonic and the Keplerian potentials is the same as that described by a Bohlin transformation [19]. In order to get a real r_1 , the quantity $\frac{\beta}{\xi_1}$ must be negative. The angle φ_0 of the Keplerian orbit is twice that of the corresponding φ_1 of the harmonic one, as represented in figure 7. The focus F of the Keplerian ellipse is the center of the harmonic one.

2. When $\alpha \neq 0$ and $\beta = 0$, then

$$\frac{d\varphi_1}{d\varphi_0} = 1.$$

The system can still be inverted as

$$\begin{cases} r_1^2 = \frac{\alpha\xi_0}{\xi_1}r_0^2, \\ \psi_1(r_1) = \alpha_1 - \frac{\mu_1}{r_1}, \end{cases} \quad \text{where } \alpha_1 = \frac{(\alpha-1)}{\alpha}\xi_1 \text{ and } \mu_1 = \mu\sqrt{\frac{\xi_1}{\alpha\xi_0}}.$$

The quantity $\frac{\xi_1}{\alpha\xi_0}$ must be positive when $x_{0,1} = 2r_{0,1}^2 > 0$. This transformation maps the primary Keplerian ellipse onto a scaled confocal one. The two moving points are always aligned with the common focus of the two ellipses. As ξ_1 needs to be negative to ensure bounded bolsted orbit, this imposes $\alpha > 0$.

These two special cases are represented in figure 7.

To show that only the harmonic and Keplerian potentials can exchange their radial orbit with a linear change of polar angles, we assume that

$$\varphi_1(t_1) = m\varphi_0(t_0) \quad \text{with } m = \text{cst.} \quad (28)$$

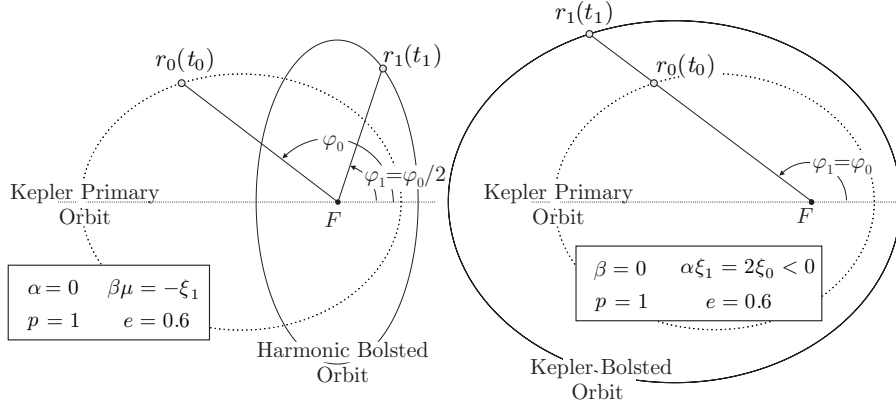


Figure 7: The transformation $B_{0,\beta}$ of a Keplerian PRO gives a harmonic PRO when $\beta\xi_1 < 0$, as represented on the left panel. The transformation $B_{\alpha,0}$ of a Keplerian PRO gives a Keplerian PRO when $\alpha > 0$ and $\xi_1 < 0$, as represented on the right panel.

Combining (23) with the derivative of (28) one can verify that y_0 satisfies the ODE

$$\frac{dy}{dx_0} - \frac{m}{x_0}y = \xi_0 \frac{\alpha}{\beta} (m-1), \quad (29)$$

which holds for $\beta \neq 0$. The solution of (29) is given by

$$y_0(x_0) = kx_0^m - \xi_0 \frac{\alpha}{\beta} x_0.$$

But y_0 must describe a parabola, so either

- $m = 1$ or $m = 0$. Then the potential is constant or constant with a gauge, and no PRO exists.
- $m = \frac{1}{2}$. Then y_0 represents a Keplerian potential up to a constant. Inserting the solution y_0 in $(\xi_1 x_1, y_1)^\top$, y_1 is a harmonic potential with a constant.
- $m = 2$. Then y_0 represents a harmonic potential up to a constant and y_1 a transvected Keplerian potential.

Let us examine now the more general case when $\alpha\beta \neq 0$. The ODE for

phases is written as

$$\frac{d\varphi_1}{d\varphi_0} = \frac{N(\varphi_0)}{D(\varphi_0)} \quad \text{where} \quad \begin{cases} N(\varphi_0) = \frac{dx_1}{dx_0} = \frac{1}{\xi_1} \left[\alpha\xi_0 - \frac{\mu\beta}{2p} (1 + e \cos \varphi_0) \right], \\ D(\varphi_0) = \frac{x_1}{x_0} = \frac{1}{\xi_1} \left[\alpha\xi_0 - \frac{\mu\beta}{p} (1 + e \cos \varphi_0) \right]. \end{cases} \quad (30)$$

We first remark that the denominator function $\varphi \rightarrow D(\varphi)$ is strictly positive as both $x_0 = 2r_0^2$ and $x_1 = 2r_1^2$ are positive functions. In (25) we have seen that the sign of $N(\varphi)$ cannot change; as a consequence the function $\varphi_0 \rightarrow \varphi_1(\varphi_0)$ is monotone. In our hypothesis where $N(\varphi) \geq 0$, φ_1 is an increasing function of φ_0 . After a little rearrangement, from (30) we obtain

$$\varphi_1 = \int_0^{\varphi_0} \frac{\eta + \cos \varphi}{\delta + 2 \cos \varphi} d\varphi \quad \text{where} \quad \eta = \frac{\mu\beta - 2p\alpha\xi_0}{\mu\beta e} \geq 1 \quad \text{and} \quad \delta = \frac{2\mu\beta - 2p\alpha\xi_0}{\mu\beta e} > 2.$$

We notice that the particular case when the primary Keplerian orbit is circular, i.e. $e = 0$, linearly links φ_0 and φ_1 . The integral for φ_1 can be made explicit: introducing $u = \tan(\varphi/2)$ we get $\cos \varphi = \frac{1-u^2}{1+u^2}$, $d\varphi = \frac{2du}{1+u^2}$ and thus

$$\varphi_1 = 2 \int_0^{u_0} \frac{\ell + 2 + \ell u^2}{(m + 4 + mu^2)(1 + u^2)} du \quad \text{where} \quad \begin{cases} \ell = \eta - 1 \geq 0, \\ m = \delta - 2 > 0. \end{cases}$$

A partial fraction decomposition gives

$$\varphi_1 = \int_0^{u_0} \frac{1}{1 + u^2} du + \frac{2\ell - m}{\sqrt{m(m+4)}} \int_0^{v_0} \frac{dv}{1 + v^2},$$

where $v = \sqrt{\frac{m}{m+4}}u$. The integration leads to

$$\varphi_1 = \frac{\varphi_0}{2} + \frac{2\ell - m}{\sqrt{m(m+4)}} \arctan \left[\sqrt{\frac{m}{m+4}} \tan \left(\frac{\varphi_0}{2} \right) \right],$$

and so

$$\varphi_1 = \frac{\varphi_0}{2} + \frac{\chi}{\sqrt{(1+\chi)^2 - e^2}} \arctan \left[\sqrt{\frac{1+\chi-e}{1+\chi+e}} \tan \left(\frac{\varphi_0}{2} \right) \right] \quad \text{with} \quad \chi = \frac{p\alpha |\xi_0|}{\mu\beta}.$$

If $\alpha = 0$ we would recover the relation $\varphi_1 = \frac{\varphi_0}{2}$ previously mentioned. In the same way, when $\beta \rightarrow 0$, then $\varphi_1 \rightarrow \varphi_0$. When the bolsted orbit is a PRO, we can easily compute the increment of the azimuthal angle $\Delta\varphi$ during the transfer from r_a to r_p and back. In the Keplerian case, from figure 8, we

see that the transfer for $r_0 : r_{0,p} \rightarrow r_{0,a}$ corresponds to $\varphi_0 : 0 \rightarrow \pi$. Hence, using (27) one gets

$$\begin{aligned} \varphi_1 : 0 \rightarrow \frac{1}{2}\Delta\varphi_1 &= \frac{\pi}{2} + \frac{\chi}{\sqrt{(1+\chi)^2 - e^2}} \arctan(\infty) \\ &= \frac{\pi}{2} \left(1 + \frac{\chi}{\sqrt{(1+\chi)^2 - e^2}} \right). \end{aligned}$$

Since

$$p = \frac{\Lambda^2}{\mu} \text{ and } e = \sqrt{1 + \frac{2\Lambda^2\xi_0}{\mu^2}},$$

we see that $\Delta\varphi_1$ depends on Λ^2 but not on ξ_1 . This is a characterization of isochrone orbits (see theorem A.1 in appendix A). Given a point (φ_0, r_0) on the primary Keplerian ellipse, its image on the bolsted orbit has a polar angle φ_1 given by the formula (27) and a distance r_1 given by the relation (24), i.e.

$$x_1 = 2r_1^2 = 2\alpha \frac{\xi_0}{\xi_1} r_0^2 - 2\mu \frac{\beta}{\xi_1} r_0 \implies r_1^2 = \frac{\alpha\xi_0 r_0^2 - \mu\beta r_0}{\xi_1}.$$

When α , β and ξ_1 are such that $r_1^2 > 0$ for all r_0 on the Keplerian orbit, this corresponds to an isochrone PRO. □

□

Theorem 3.1 shows that any Keplerian PRO can be transformed into a particular isochrone one by a suitable bolst $B_{\alpha,\beta}$. When $\alpha = 0$, the bolst coincides with a Bohlin transformation. In the other cases, it generalizes it; we have plotted an example of such a bolst in figure 8.

Reciprocally, we will see in sec. 3.2.5 that any isochrone PRO could be connected to a Keplerian ellipse.

3.1.3 The bolst, a key to isochrony

Geometrically, a Keplerian parabola in a frame $\mathcal{R}_O = (O, \vec{i}, \vec{j})$ is laid (see sec. 2.2, p. 13), i.e. its tangent at the origin is $\mathbb{R}\vec{j}$ and its axis of symmetry is $\mathbb{R}\vec{i}$. According to lemma C.2 in appendix C, its image by a bolst $B_{\alpha,\beta}$ remains laid, and so Keplerian, in the image frame $B_{\alpha,\beta}(\mathcal{R}_O)$. But, in \mathcal{R}_O , the image parabola has two distinct intersections with $\mathbb{R}\vec{j}$ and thus appears to be a non-Keplerian isochrone. Therefore, it appears that to be or not to be Keplerian depends on the choice of the reference frame. This is an aspect of the isochrone relativity that we will discuss in what follows.

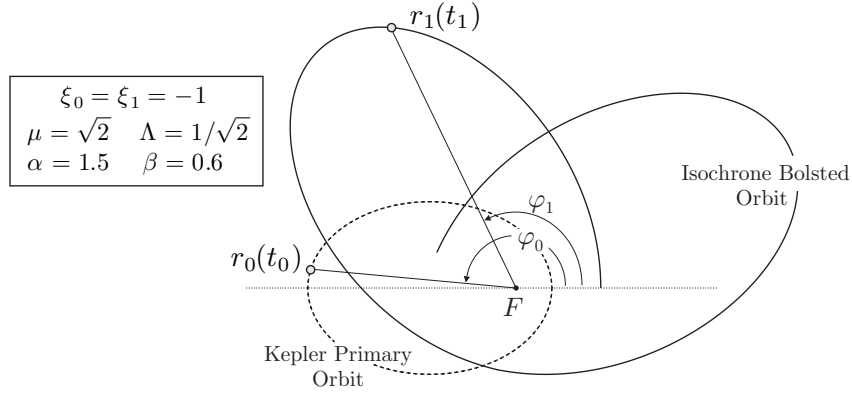


Figure 8: The $\alpha = 1.5$ and $\beta = 0.6$ bolst of a Keplerian ellipse ($e \simeq 0, 7$; $p \simeq 0.35$) which gives an isochrone orbit with the same energy ($\xi_0 = \xi_1 = -1$).

For this discussion, we will not consider the general case of any bolst $B_{\alpha,\beta}$. With only technical restrictions, we will consider the case where the bolst is symmetric: according to (24), $B_{\alpha,\beta}$ is a symmetric matrix if and only if $\alpha - 1 = \beta$. Introducing the parameter $\gamma = \alpha + \beta$ which is the variable eigenvalue of $B_{\alpha,\beta}$, with the other 1, the general bolst $B_{\alpha,\beta}$ then becomes the symmetric B_γ that we call an *ibolst* for which the isochrone relativity appears to be clear.

We have seen that bolsts generalize the Bohlin transformation, and we will see now that ibolsts are the boosts of the isochrone relativity. Names appear to be clarified: *bolst* stands for bohlin boost and *ibolst* for symmetric bohlin boost.

3.2 Isochrone relativity

The special theory of relativity has two pillars:

1. The Einstein principle of special relativity imposes that the laws of physics can be written in the same way in all Galilean frames;
2. The length of any space-time interval is conserved through changes of Galilean frames, aka Lorentz frames.

These principles make time and length relative to a given Galilean frame. These two physical quantities are linearly exchanged during changes of Galilean frames.

In the same way, the linear exchange between ξx and y proposed in the previous section conserves the “*isochrone interval*” $\xi x - y$ in equation (22). This conservation is imposed by that of the fundamental orbital law (19) which renders the conservation of the energy along the orbit. The linearity of the transformation is associated with the isochrony preservation. The conservations of the “*isochrone interval*” and isochrone law are the two pillars of the isochrone relativity.

For the sake of simplicity, we restrict our attention to symmetric exchanges between ξx and y : the bolst $B_{\alpha,\beta}$ is then reduced to the ibolst $B_{\gamma=\alpha+\beta}$, choosing $\alpha - 1 = \beta$,

$$B_\gamma = \frac{1}{2} \begin{bmatrix} \gamma + 1 & \gamma - 1 \\ \gamma - 1 & \gamma + 1 \end{bmatrix}.$$

3.2.1 The ibolst Algebra

Let $\mathcal{R} = (\vec{i}, \vec{j})$ be the canonical basis of \mathbb{R}^2 . Any vector $\vec{z} \in \mathbb{R}^2$ has affine coordinates (z_1, z_2) in the frame $\mathcal{R}_O = (O, \vec{i}, \vec{j})$, i.e. there exists a unique point Z in the Oz_1z_2 plane such that $\vec{z} = \overrightarrow{OZ} = z_1\vec{i} + z_2\vec{j}$. We do not use the usual upper index for contravariant components because, as we are in \mathbb{R}^2 , we do not use Einstein notation for sums and we prefer to conserve the upper index for powers. The orthonormality is defined in the Euclidian sense, i.e. with natural notations

$$\|\vec{z}\|^2 = (\vec{z}|\vec{z}) = z_1^2 + z_2^2 \text{ then } (\vec{i}|\vec{i}) := \|\vec{i}\|^2 = \|\vec{j}\|^2 =: (\vec{j}|\vec{j}) = 1 \text{ and } (\vec{i}|\vec{j}) = 0.$$

The \mathcal{R} basis is then orthonormal for the Euclidian scalar product. We will also use the Minkowski scalar product for which

$$\|\vec{z}\|_m^2 = \langle \vec{z}|\vec{z} \rangle = z_1^2 - z_2^2 \text{ then } \langle \vec{i}|\vec{i} \rangle := \|\vec{i}\|_m^2 = 1, \quad \langle \vec{j}|\vec{j} \rangle := \|\vec{j}\|_m^2 = -1 \text{ and } \langle \vec{i}|\vec{j} \rangle = 0.$$

Consider the two eigenvectors $\vec{k} = \frac{1}{\sqrt{2}}(\vec{i} - \vec{j})$ and $\vec{l} = \frac{1}{\sqrt{2}}(\vec{i} + \vec{j})$ of the ibolst B_γ such that

$$B_\gamma(\vec{k}) = \vec{k} \text{ and } B_\gamma(\vec{l}) = \gamma\vec{l}. \quad (31)$$

The basis $\tilde{\mathcal{R}} = (\vec{k}, \vec{l})$ is just \mathcal{R} rotated by an angle of $-\frac{\pi}{4}$. It is thus orthonormal for the Euclidian scalar product. Moreover, we see that for the Minkowski scalar product, we have

$$\langle \vec{k}|\vec{k} \rangle = \langle \vec{l}|\vec{l} \rangle = 0 \text{ and } \langle \vec{k}|\vec{l} \rangle = \langle \vec{l}|\vec{k} \rangle = 1. \quad (32)$$

From (31), let us remark that the set $\mathbb{B} = \{B_\gamma, \gamma \in \mathbb{R}^*\}$ forms a commutative linear group since

$$\forall (\gamma, \gamma') \in \mathbb{R}^* \times \mathbb{R}^*, \quad B_\gamma \circ B_{\gamma'} = B_{\gamma'} \circ B_\gamma = B_{\gamma\gamma'} \in \mathbb{B}.$$

For this law, B_1 is an identity element. The inverse of a transformation B_γ for $\gamma \in \mathbb{R}^*$ is $B_{\frac{1}{\gamma}}$.

As expected, any ibolst is symmetric, i.e. for the Euclidian scalar product and for any vectors \vec{w} and \vec{z} , we have

$$(B_\gamma(\vec{w}) | \vec{z}) = (\vec{w} | B_\gamma(\vec{z})). \quad (33)$$

As a matter of fact, since the matrix B_γ is symmetric, considering the expansion of these vectors in the basis $\tilde{\mathcal{R}}$ noted with a tilde, we get directly from (31) that

$$\begin{aligned} (B_\gamma(\vec{w}) | \vec{z}) &= \left(\tilde{w}_1 B_\gamma(\vec{k}) + \tilde{w}_2 B_\gamma(\vec{l}) \mid \tilde{z}_1 \vec{k} + \tilde{z}_2 \vec{l} \right) = \tilde{w}_1 \tilde{z}_1 + \gamma \tilde{w}_2 \tilde{z}_2 \\ &= \tilde{z}_1 \tilde{w}_1 + \gamma \tilde{z}_2 \tilde{w}_2 = (B_\gamma(\vec{z}) | \vec{w}) = (\vec{w} | B_\gamma(\vec{z})). \end{aligned}$$

However this symmetry property does not generally hold for the Minkowski scalar product.

3.2.2 Lengths and spaces

Let us consider ξ and Λ as two fixed parameters. We can define in \mathcal{R}_O the affine coordinates system ($w_1 = \xi x, w_2 = y$). Using these coordinates we set

$$\vec{w}' = B_\gamma(\vec{w}).$$

The symmetry (33) of the ibolst for the Euclidian scalar product gives

$$\forall \alpha \in \mathbb{R}, \quad (\vec{w}' | \alpha \vec{l}) = (B_\gamma(\vec{w}) | \alpha \vec{l}) = (\vec{w} | B_\gamma(\alpha \vec{l})) = \gamma (\vec{w} | \alpha \vec{l}).$$

With $\alpha = \sqrt{2}$, this relation corresponds to the equality

$$\xi' x' + y' = \gamma (\xi x + y). \quad (34)$$

This same symmetry, but in the direction given by \vec{k} , gives the conservation of the isochrone interval

$$\forall \alpha \in \mathbb{R}, \quad (\vec{w}' | \alpha \vec{k}) = (\vec{w} | \alpha \vec{k}) \Rightarrow \xi' x' - y' = \xi x - y. \quad (35)$$

By multiplication of these two relations we get directly⁴

$$(\xi'x')^2 - y'^2 = \gamma \left[(\xi x)^2 - y^2 \right]. \quad (36)$$

This relation corresponds to the fact that an ibolst is not an isometry using the Minkowskian norm

$$\langle \vec{w}' | \vec{w}' \rangle = \gamma \langle \vec{w} | \vec{w} \rangle. \quad (37)$$

As a consequence, the radial cone

$$\mathcal{C} = \{ \vec{z} \in \mathbb{R}^2, \langle \vec{z} | \vec{z} \rangle = 0 \}$$

is preserved by the ibolst as $\mathcal{C} = \mathbb{R}\vec{k} \cup \mathbb{R}\vec{l}$. Its name comes from the fact that the line $y = \xi x$ defines a radial orbit ($\Lambda = 0$) of energy ξ in the potential $\psi(r)$. In a Kepler potential $\psi_{\text{ke}}(r) = -\frac{\mu}{r}$ a test particle of energy $\xi < 0$ with a radial orbit moves on a segment from $r_a = \frac{\mu}{|\xi|}$ at $t = 0$ to $r \rightarrow 0$ when $t \rightarrow +\infty$. As its period should be infinite, a radial orbit is not a PRO but we can say that it is a maximal time-bounded orbit.

In this relativistic formulation of the problem we can then define periodic-like vectors lying in the periodic space

$$\mathcal{P} = \{ \vec{z} \in \mathbb{R}^2, \langle \vec{z} | \vec{z} \rangle < 0 \}$$

and aperiodic-like vectors lying in the aperiodic space

$$\mathcal{A} = \{ \vec{z} \in \mathbb{R}^2, \langle \vec{z} | \vec{z} \rangle > 0 \}.$$

As the convex x -positive part of parabolas containing PRO in the coordinates system $(\xi x, y)$ is delimited by the radial cone and exactly contained in \mathcal{P} , the names \mathcal{P} and \mathcal{A} are natural.

3.2.3 Orbits relativity

Let us define the ibolsted frame $\mathcal{R}'_O = (O, \vec{u}, \vec{v})$ such that

$$\left\{ \begin{array}{l} \vec{u} = B_\gamma \left(\begin{array}{c} \vec{i} \\ \vec{j} \end{array} \right) = B_\gamma \left(\frac{\vec{l} + \vec{k}}{\sqrt{2}} \right) = \frac{\gamma \vec{l} + \vec{k}}{\sqrt{2}} \\ \text{and} \\ \vec{v} = B_\gamma \left(\begin{array}{c} \vec{i} \\ \vec{j} \end{array} \right) = B_\gamma \left(\frac{\vec{l} - \vec{k}}{\sqrt{2}} \right) = \frac{\gamma \vec{l} - \vec{k}}{\sqrt{2}} \end{array} \right. \implies \vec{k} = \frac{\vec{u} - \vec{v}}{\sqrt{2}}. \quad (38)$$

⁴The relation (35) holds for any bolst $B_{\alpha,\beta}$. This is not the case for (34) which requires the B_γ -symmetry. As a consequence, the relation (36) is simple only in the symmetric case.

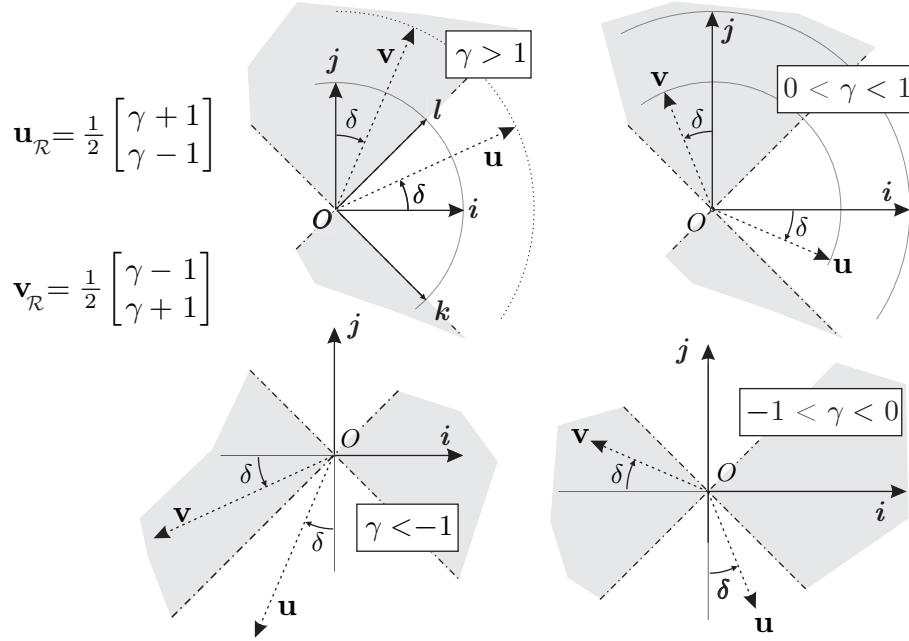


Figure 9: The bolsted frame $\mathcal{R}'_O = (O, \vec{u}, \vec{v})$, when $\xi\xi' > 0$. Its periodic space \mathcal{P}' is represented in grey, while its aperiodic one \mathcal{A}' is in white.

Definition 3.1. *The reference frame of a given parabola \mathcal{P} is the frame (O, \vec{t}, \vec{n}) where the tangent to the parabola at the origin is $\mathcal{T}_O(\mathcal{P}) = \mathbb{R}\vec{t}$ and the symmetry axis is $\mathcal{S}(\mathcal{P}) = \mathbb{R}\vec{n}$.*

A reference frame geometrically defines a parabola up to a scale factor. For instance, \mathcal{R}_O is the reference frame of the Keplerian parabola containing ψ_{ke} up to the scale factor μ . According to lemma C.2 in appendix C, the line $\mathbb{R}\vec{v}$ is tangent to the bolsted parabola and $\mathbb{R}\vec{u}$ is its symmetry axis. Thus, \mathcal{R}'_O is the reference frame of the bolsted parabola and characterizes it up to a scale factor.

All possibilities are represented in figure 9, when the primary energy ξ and the image energy ξ' share the same sign. When $\xi\xi' < 0$, the direction of \vec{u} has to be inverted.

Depending on the value of $\gamma \neq 1$, we can define the angle δ given by

$$\tan \delta = \left| \frac{\gamma + 1}{\gamma - 1} \right|$$

which is useful to construct \mathcal{R}'_O from \mathcal{R}_O by simple composition of a homothety and a hyperbolic rotation (see [8] p.28 for a nice description in French or [16] for general properties of rotation in special relativity).

As with \vec{i} and \vec{j} , the two ibolsted basis vectors \vec{u} and \vec{v} have the same Euclidian norm

$$\|\vec{u}\|^2 = \|\vec{v}\|^2 = \frac{\gamma^2 + 1}{2}$$

and opposed Minkowskian lengths

$$\|\vec{u}\|_m = \gamma = -\|\vec{v}\|_m.$$

Moreover, from (32) and (38), the primary and the ibolsted basis are orthogonal in the Minkowskian scalar product: $\langle \vec{i} | \vec{j} \rangle = \langle \vec{u} | \vec{v} \rangle = 0$. Depending on γ and on the frame \mathcal{R}_O or \mathcal{R}'_O used to define the scalar product, one vector is aperiodic-like and the other is periodic-like, see figure 9.

In the canonical frame \mathcal{R}_O , using the isochrone relativity formalism and introducing the proper time $d\tau = \xi dt$ of an orbit of energy ξ and angular momentum Λ , the orbital differential equation (19) in the affine coordinates $(\xi x, y)$ can be written as

$$\frac{1}{16} \left[\frac{d}{d\tau} (\vec{w} | \vec{i}) \right]^2 = (\vec{w} | \vec{i} - \vec{j}) + (\vec{w}_\Lambda | \vec{j}), \quad (39)$$

where $\vec{w}_\Lambda = -\Lambda^2 \vec{j}$. The vector \vec{w} describes the potential of parabola \mathcal{P} and the orbit which corresponds to an arc of \mathcal{P} . When this orbit is a PRO, this arc is finite. When \vec{w} describes a Keplerian orbit, its ibolsted image \vec{w}' is characterized by theorem 3.2.

Theorem 3.2. *A vector \vec{w}' describes an isochrone orbit (ξ', Λ') on its arc of parabola if and only if it is the image, by an ibolst $B_\gamma \in \mathbb{B}$, of a vector \vec{w} which describes a Keplerian orbit (ξ, Λ) on a Keplerian parabola. In the Keplerian frame $\mathcal{R}_O = (O, \vec{i}, \vec{j})$, the orbit (ξ', Λ') is isochrone but generally not Keplerian. In its natural bolsted frame $\mathcal{R}'_O = (O, \vec{u}, \vec{v})$ it is a Keplerian orbit with angular momentum Λ . If $\xi \xi' > 0$ then⁵*

$$\Lambda' = \sqrt{\gamma} \Lambda$$

else

$$\Lambda' = \Lambda.$$

⁵When $\gamma < 0$, Λ is imaginary and does not correspond to a PRO.

Proof. In the affine coordinate system $(w_1 = |\xi|x, w_2 = y)$, an orbit of energy $\xi < 0$ and angular momentum Λ corresponds to an arc of the parabola \mathcal{P} . When this orbit is a PRO, the two extremities A and P of this parabolic arc are associated with the two solutions apoastron \vec{w}_A and periastron \vec{w}_P of the equation $\frac{d}{d\tau}(\vec{w}, \vec{i}) = 0$, with $d\tau = |\xi|dt$. Considering the orbital differential equation (39) in the coordinates $(|\xi|x, y)$, these two extremal points of the orbit are on the extremal line

$$\Delta = \left\{ \vec{w} \in \mathbb{R}^2, \sqrt{2}(\vec{w}|\vec{k}) = \Lambda^2 \right\}.$$

Trivially we then note that Δ is parallel to $\mathbb{R}\vec{k}$. As the vectors \vec{w} defining this PRO satisfy $\left[\frac{d}{d\tau}(\vec{w}, \vec{i}) \right]^2 \geq 0$, they are periodic-like vectors. Defining

$$K = \mathcal{T}_O(\mathcal{P}) \cap \Delta,$$

the point K is the \vec{k} parallel projection of A and P on $\mathbb{R}\vec{j}$ and trivially,

$$\overrightarrow{OK} = -\Lambda^2 \vec{j}. \quad (40)$$

When $\gamma > 1$, the ibolst of the Kepler parabola is represented in figure 10; the other values of γ can be deduced directly from figure 9 and the analysis we will give below. With natural notations, we set $\mathcal{P}' = B_\gamma(\mathcal{P})$ and $\Delta' = B_\gamma(\Delta)$. As Δ is parallel to $\mathbb{R}\vec{k}$, which is an invariant direction of the ibolst, Δ' is also parallel to $\mathbb{R}\vec{k}$. Let us consider $K' = B_\gamma(K)$. According to lemma C.2 we have

$$\begin{aligned} K' &= B_\gamma(\mathcal{T}_O(\mathcal{P}) \cap \Delta) \\ &= B_\gamma(\mathcal{T}_O(\mathcal{P})) \cap B_\gamma(\Delta) \\ &= \mathcal{T}_O(\mathcal{P}') \cap \Delta' \end{aligned}$$

and quantitatively, as $\overrightarrow{OK} = -\Lambda^2 \vec{j}$, after an ibolst, we get

$$\overrightarrow{OK'} = -\Lambda^2 \vec{v}. \quad (41)$$

This relation clearly indicates that Λ is the same angular momentum for the Keplerian orbit and for the ibolsted orbit when it is considered in the reference frame of its ibolsted parabola, where it is also a Keplerian one. In addition,

$$\Delta' = K' + \mathbb{R}\vec{k} = B_\gamma(K) + \mathbb{R}B_\gamma(\vec{k}). \quad (42)$$

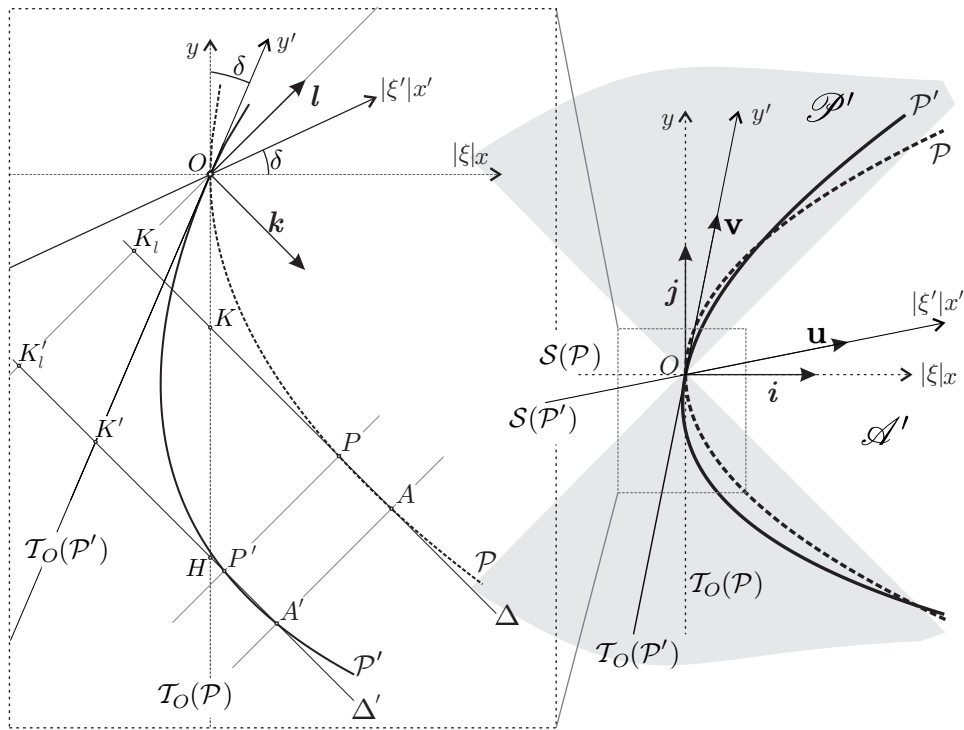


Figure 10: The $\gamma > 1$ ibolst of the Kepler parabola when $\xi\xi' > 0$.

Therefore, each point of the isochrone orbit on its arc of parabola is directly linked by the ibolst to its \vec{l} -parallel projection on the Keplerian parabola . We can determine the angular momentum Λ' of the isochrone orbit in the Keplerian coordinates. Combining (38), (40) and (41) we get

$$\overrightarrow{KK'} = -\Lambda^2 (\vec{v} - \vec{j}) = -\frac{\Lambda^2}{\sqrt{2}} (\gamma - 1) \vec{l}.$$

If we introduce now the two orthogonal projections K_l and K'_l of K and K' on $\mathbb{R}\vec{l}$, we have $\overrightarrow{KK'} = \overrightarrow{K_lK'_l}$ and $\overrightarrow{OK'_l} = B_\gamma(\overrightarrow{OK_l})$ by (42). Since $K_l = \Delta \cap \mathbb{R}\vec{l}$, $K'_l = \Delta' \cap \mathbb{R}\vec{l}$ and B_γ sends Δ to Δ' and \vec{l} to $\gamma\vec{l}$, we get

$$\overrightarrow{OK'_l} = B_\gamma(\overrightarrow{OK_l}) = \gamma \overrightarrow{OK_l}.$$

And finally by Thales theorem,

$$\frac{OK'_l}{OK_l} = \frac{OH}{OK} = \gamma \quad \text{where } H = \mathcal{T}_O(\mathcal{P}) \cap \Delta'. \quad (43)$$

The length OH is the squared angular momentum Λ'^2 of the ibolsted orbit considered in the reference frame of the Keplerian parabola. As OK is the squared angular momentum of the Keplerian orbit in its natural frame, we have

$$\Lambda'^2 = \gamma \Lambda^2.$$

When $\xi\xi' < 0$, the orientation of \vec{u} is inverted. The line Δ' is $\Delta' = K' + \mathbb{R}\vec{l}$, and since $\overrightarrow{OK'_l}$ is directed by \vec{k} , then $\Lambda' = \Lambda$. □

□

The bolsted orbital differential equations follow from theorem 3.2. As we can see from (45), in isochrone relativity, orbital laws are the same in all reference frames.

Corollary 3.2.1. *In the canonical frame \mathcal{R}_O , the bolsted orbital differential equation is*

$$\frac{1}{16} \left[\frac{d}{d\tau} \left(\vec{w}' | \vec{i} \right) \right]^2 = \left(\vec{w}' | \vec{i} - \vec{j} \right) + \left(\vec{w}'_{\Lambda'} | \vec{j} \right) \quad (44)$$

with $\vec{w}'_{\Lambda'} = -\Lambda'^2 \vec{j}$.

In the bolsted frame \mathcal{R}'_O with affine coordinates $(\xi'x', y')$ and proper time $d\tau' = \xi' dt'$, the bolsted orbital differential equation is

$$\frac{1}{16} \left[\frac{d}{d\tau'} \left(\vec{w}' | \vec{u} \right) \right]^2 = \left(\vec{w}' | \vec{u} - \vec{v} \right) + \left(\vec{w}'_{\Lambda'} | \vec{v} \right) \quad (45)$$

with $w'_\Lambda = -\Lambda^2 \vec{v}$.

Isochrone PRO are contained in the periodic-space of their parabola reference frame. But in the Keplerian primary frame this periodic-space appears vertical when $\gamma > 0$ and horizontal otherwise. In some cases, the PRO is then associated with an arc of parabola which is concave or located in the negative part of the Keplerian frame. Those image orbits are not physical.

3.2.4 Potentials relativity

The Keplerian nature of an isochrone potential is revealed in the reference frame \mathcal{R}'_O of its parabola, cf theorem 3.2. An ibolst can also bolst a harmonic potential and then exactly provide the appropriate primary frame which characterizes the radial oscillation of a PRO in the image isochrone potential. In such a frame, all periods of PRO have indeed the same value.

We give hereafter an explicit formulation of the parameters of all the image potentials. They can be obtained by direct resolution of quadratic equations.

When the primary potential is Keplerian $\psi_{\text{ke}}(r) = -\frac{\mu}{r}$, the primary orbits are such that $\xi < 0$ in order to be bounded. If $\gamma > 0$, the ibolsted potential $\psi'(r')$ is always a transvection of a Hénon or a bounded isochrone potential introduced in sec. 2.3. Using the notations of reduced potentials, coming from the proof of theorem 2.5 and equation (16), one can verify that

	$\text{sign}(\xi') = -\text{sign}(\xi) > 0$	$\text{sign}(\xi') = \text{sign}(\xi) < 0$
$\gamma > 1$	$J_{\epsilon,0}(\psi_{\text{bo}}^+) = \psi_{\text{bo}}^+ + \epsilon$	$J_{\epsilon,0}(\psi_{\text{he}}^-) = \psi_{\text{he}}^- + \epsilon$
$0 < \gamma < 1$	$J_{-\epsilon,0}(\psi_{\text{bo}}^-) = \psi_{\text{bo}}^- - \epsilon$	$J_{-\epsilon,0}(\psi_{\text{he}}^+) = \psi_{\text{he}}^+ - \epsilon$

(46)

where

$$\epsilon = \frac{\mu'(\gamma+1)^2}{8\gamma b} > 0, \quad \mu' = \left| \frac{8\mu\xi'\gamma}{(\gamma+1)\sqrt{|8\xi\xi'(\gamma+1)|}} \right| \quad \text{and} \quad b = \left| \frac{\mu(\gamma-1)}{\sqrt{|8\xi\xi'(\gamma+1)|}} \right|.$$

Then, when the primary potential $\psi(r)$ is the harmonic $\psi_{\text{ha}}(r) = +\frac{1}{2}\omega^2 r^2$, the primary energy is positive $\xi > 0$ in order to get bounded orbits. When

$\gamma > 0$, the ibolst leads to the four increasing potentials $\psi'(r')$,

	$\text{sign}(\xi') = \text{sign}(\xi) > 0$	$\text{sign}(\xi') = -\text{sign}(\xi) < 0$
$\gamma > 1$	$J_{\epsilon,0}(\psi_{\text{he}}^+) = \psi_{\text{he}}^+ + \epsilon$	$J_{\epsilon,0}(\psi_{\text{bo}}^-) = \psi_{\text{he}}^+ + \epsilon$
$0 < \gamma < 1$	$J_{-\epsilon,0}(\psi_{\text{bo}}^+) = \psi_{\text{bo}}^+ - \epsilon$	$J_{-\epsilon,0}(\psi_{\text{bo}}^+) = \psi_{\text{bo}}^+ - \epsilon$

(47)

where

$$\epsilon = \frac{\mu'(\gamma-1)^2}{8b\gamma}, \quad \mu' = \left| \frac{4\xi'\xi\gamma}{\omega(\gamma-1)\sqrt{|\xi'(\gamma-1)|}} \right| \quad \text{and} \quad b = \frac{(\gamma+1)|\xi|}{2\omega\sqrt{|\xi'(\gamma-1)|}}.$$

The classical Bohlin transformation B_{-1} exchanges the two potentials ψ_{ke} and ψ_{ha} , cf. theorem 3.1 p.26. The commutative structure and associative property of the group \mathbb{B} then provide the image of any isochrone potential by B_γ when $\gamma < 0$.

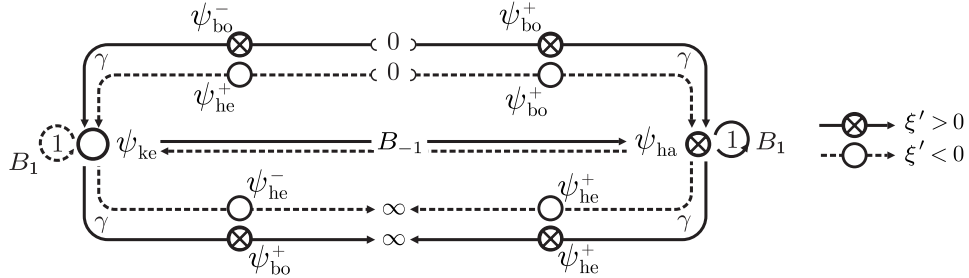


Figure 11: Diagram of the set of all possible ibolsted potentials up to an additive constant. The nomenclature used is the one defined in the isochrone classification of sec. 2.3.

A transvection $J_{\epsilon,0}$ swivels a parabola when it only adds the constant ϵ to the corresponding potential. This constant has no particular role and we can neglect it in a potential diagram summarizing the effect of the ibolst on isochrone potentials. This is the purpose of figure 11.

Using this diagram and the group property of the ibolst, we can recover all ibolsted potentials only from the Keplerian one. Isochrone potentials form the group orbit of Kepler potentials under the action of \mathbb{B} .

3.2.5 Isochrone orbits construction

Isochrony is a Keplerian property seen from an appropriate reference frame. Theorem 3.2 gives a method to find the relative isochrone reference frame from a Keplerian potential. From any isochrone potential one may reciprocally construct its isochrone orbits and find their related Keplerian description graphically using parabolas.

In order to be concrete, we build now the complete *back to the Kepler* process when the needed ibolst has $\gamma > 1$ for $\xi\xi' > 0$ in figure 12.

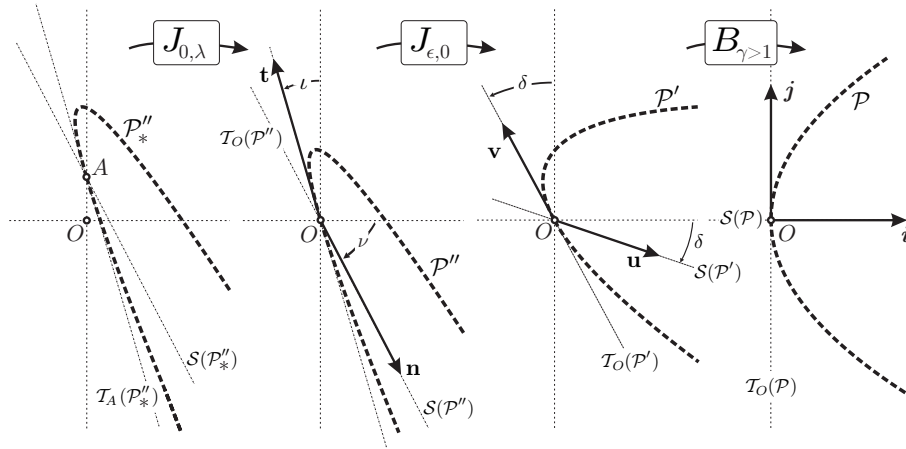


Figure 12: Graphical determination of the Keplerian reference frame of an isochrone parabola. Here isochrone orbits have negative energy.

Consider a parabola \mathcal{P}_*'' . From definition 2.2 p.19, we retrieve a *physical* parabola from a vertical translation $J_{0,\lambda}(\mathcal{P}_*'') = \mathcal{P}''$. Then, by definition 3.1 p.35, we find the natural frame (O, \vec{t}, \vec{n}) attached to \mathcal{P}'' . While the angles ι and ν are not equal, we adjust the parabola with a transvection $J_{\epsilon,0}$ to prepare it for a bolst. We then debolst the parabola with the ibolst B_γ given by the angle $\delta = \iota = \nu$, with $\delta < \frac{\pi}{2}$. Given \mathcal{P} and \mathcal{P}' , the isochrone orbit can be related to its Keplerian description as in figure 10.

This geometrical construction gives the radial distances

$$r_0 = \frac{1}{2\sqrt{|\xi_0|}} \sqrt{(\vec{w}|\vec{i})} \quad \text{and} \quad r_1 = \frac{1}{2\sqrt{|\xi_0|}} \sqrt{(\vec{w}'|\vec{i})}$$

of the Keplerian and isochrone orbits in the $(|\xi_0|x, y)$ -coordinates of the Keplerian frame. The angles φ_0 and φ_1 are provided by theorem 3.1 p.26

and given by

$$a = \frac{1}{2}(r_{0,p} + r_{0,a}), \quad \frac{|\xi_0|}{\mu} = \frac{1}{2a}, \quad e = \frac{r_{0,a} - r_{0,p}}{2a}, \quad p = (1 - e^2)a, \quad \text{and} \quad \frac{\alpha}{\beta} = \frac{\gamma + 1}{\gamma - 1}.$$

They can also be geometrically determined. In fact, the precession of the isochrone apocenters or pericenters n_φ depends on Λ and the ordinate of the intersection of the convex part of the parabola and $\mathbb{R}\vec{j}$, see proposition 4.0.1. This intersection is given by the vertical translation parameter λ and the aperture of the parabola; more precisely, by the distance $4b\mu$ between the two intersections of the parabola and the axis $\mathbb{R}\vec{j}$, just as one can deduce from (16) and its following properties on page 18.

This construction does not explicitly depend on the hypothesis $\gamma > 1$, and can be generalized to other values of γ as long as the considered initial orbit is a PRO, i.e. \vec{w}' remains a periodic-like vector on the convex part of a parabola. It is also possible to construct positive energy ibolsted orbits from negative energy Keplerian orbits.

This procedure can also be generalized using a bolst $B_{\alpha,\beta}$, which is a transvection of an ibolst B_γ when expressed in the basis (\vec{l}, \vec{k}) . In the same way, the first translation $J_{0,\lambda}$ is not compulsory.

4 Applications

4.1 Physical properties of isochrone potentials

Up to an affine transformation, there are four different increasing potentials which are isochrone, i.e. in which the radial periods τ_r only depend on the energy of the considered radially oscillating particles. Two of them are very well known: the Kepler potential ψ_{ke} is associated with a Dirac density distribution and the harmonic potential ψ_{ha} is sourced by a constant density distribution of matter in the considered volume. In figure 13 we present the plot of the two other ones, i.e. ψ_{bo} and ψ_{he} . Notice their harmonic quadratic behavior at small radial distances.

The Hénon potential ψ_{he} has important physical properties in gravitational stellar dynamics: in a forthcoming paper in preparation by Simon-Petit et al., we will show that it appears to be a fundamental equilibrium state where stellar systems settle down after violent relaxation (e.g. [28] for the original contribution and [6] p. 380-382 for a modern review). The corresponding density is a core-halo structure: the typical

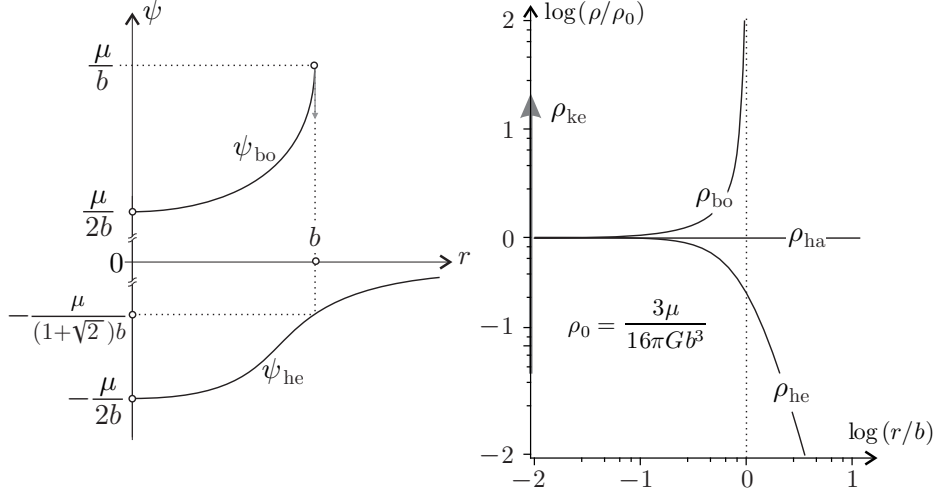


Figure 13: The bounded and the Hénon isochrone potential (left). The mass density of isochrones (right).

size of the core is the length b and the surrounding halo falls like a r^{-4} power law. This property ensures that the mass $M_{he}(r)$ contained in any ball of radius r in a Hénon potential is finite. As a matter of fact, by Gauss' theorem, we have $GM_{he}(r) = r^2 \frac{d\psi_{he}}{dr}$ and $\lim_{r \rightarrow \infty} GM_{he}(r) = \mu$. Recalling definition 2.2, this finite mass property is trivially conserved for the reduced version of the Hénon potential $\psi_{he}^{red} = \psi_{he}^+ = \psi_{he} + \frac{\mu}{2b}$ and for all physical Hénon's $\psi_{he}^{phy} = \psi_{he} + \epsilon$ for any real ϵ . However, the gauged Hénon $\psi_{he}^{gau} = \psi_{he}^{phy} + \frac{\lambda}{2r^2}$ contains an infinite mass in its center and has poor physical meaning. Nevertheless, this latter potential is still isochrone. As we said in the classification of the sec. 2.3, gauged potentials are essential for the completeness of the isochrone set.

The properties of systems associated with the ψ_{bo} potential are more unusual. When it is considered on its whole domain $\mathcal{D}_{\psi_{bo}} = [0, b]$, the systems have an infinite total mass. As a matter of fact, $GM_{bo}(r) \sim \mu \sqrt{\frac{b}{2(b-r)}}$ when $r \rightarrow b$. This property holds for any physical bounded potential. In fact these systems are self-confined because there exists an infinite repulsive force at their boundaries in $r = b$. Perhaps ψ_{bo} potentials might be used as classical models for structurally confined systems like, for example, quarks in the nucleon. Indeed, such fundamental particles are confined in the nucleon (here of size b) and are characterized by asymptotic freedom, i.e. they do not feel any force at the center of the nucleon. Gauged

bounded potentials are even more unusual with their infinite central mass!

The repartition of mass in physical isochrones is progressive: the mass is concentrated into a point in the center of a Kepler system, while in a Hénon one, the mass is equally distributed up to a characteristic length settled by the parameter b , and in a less concentrated decreasing repartition after the characteristic radius. When b increases, the first dense harmonic part grows and the Hénon potential eventually behaves like a harmonic potential since

$$\psi_{\text{he}}^{\text{red}} \underset{b \rightarrow \infty}{\sim} \frac{\mu}{8b^3} r^2, \quad (48)$$

i.e. the physical Hénon isochrone is changed into the physical harmonic when $b \rightarrow +\infty$. This property can be easily seen on the mass density distribution in the right panel of the figure 13. Subsequently, since

$$\psi_{\text{bo}}^{\text{red}} \underset{b \rightarrow \infty}{\sim} \frac{\mu}{8b^3} r^2 \quad (49)$$

we can say in a converse manner that when the infinite mass of the unbounded harmonic is concentrated into a finite domain of size b . We can recover the bounded isochrone by controlling b .

Let us revisit the properties of orbits.

4.2 Period and precession of periastron for isochrones

Proposition 4.0.1 gathers the properties τ_r and n_φ of isochrone orbits and reveals the interesting similarities of isochrone radial periods. Their form in ψ_{he} and ψ_{bo} is the same as in the Keplerian potential. We will use this remark to generalize Kepler's third law in the next subsection. In a harmonic potential, τ_r is the same regardless of the energy of the massive particles. Moreover, in ψ_{ke} and ψ_{ha} , n_φ is rational and all orbits are closed.

Proposition 4.0.1. *Given a PRO (ξ, Λ) in an isochrone potential, its radial and azimuthal periods are*

	ψ_{ke}	ψ_{ha}	ψ_{he}	ψ_{bo}	
τ_r	$2\pi\mu 2\xi ^{-3/2}$	$\pi\omega^{-1}$	$2\pi\mu 2\xi ^{-3/2}$	$2\pi\mu 2\xi ^{-3/2}$	(50)
n_φ	1	$\frac{1}{2}$	$\frac{1}{2} + \frac{\Lambda}{2\sqrt{4b\mu + \Lambda^2}}$	$\frac{1}{2} - \frac{\Lambda}{2\sqrt{4b\mu + \Lambda^2}}$	

Proof. Using isochrone potential expressions, the radial period (2) and increment n_φ of the azimuthal angle (4) come from the computation of the radial action

$$\mathcal{A}_r = \frac{1}{\pi} \int_{r_p}^{r_a} \sqrt{2[\xi - \psi(r)] - \frac{\Lambda^2}{r^2}} dr.$$

For a Keplerian orbit of energy $\xi_k < 0$ in $\psi_{\text{ke}}(r) = -\frac{\mu}{r}$ and a harmonic orbit of energy $\xi_h > 0$ in $\psi_{\text{ha}}(r) = \frac{1}{2}\omega^2 r^2$, we have

$$\mathcal{A}_r^{\text{ke}} = \frac{\sqrt{2|\xi_k|}}{\pi} \int_{r_p}^{r_a} \frac{\sqrt{(r-r_p)(r_a-r)}}{r} dr \quad \text{with} \quad \begin{cases} r_p + r_a = \frac{\mu}{|\xi_k|} \\ r_p r_a = \frac{\Lambda^2}{2|\xi_k|} \end{cases} \quad (51)$$

and

$$\mathcal{A}_r^{\text{ha}} = \frac{\sqrt{\mu}}{2\pi} \int_{r_p^2}^{r_a^2} \frac{\sqrt{(u-r_p^2)(r_a^2-u)}}{u} du \quad \text{with} \quad \begin{cases} r_p^2 + r_a^2 = \frac{2\xi_h}{\omega^2} \\ (r_p r_a)^2 = \frac{\Lambda^2}{\omega^2}. \end{cases} \quad (52)$$

The computation of these radial actions can be done by meticulous integration to recover τ_r and n_φ in ψ_{ke} and ψ_{ha} . Conversely, knowing the radial and azimuthal periods, one recovers the expression of $\mathcal{A}_r^{\text{ke}}$ and $\mathcal{A}_r^{\text{ha}}$. Indeed, for ψ_{ke} , τ_r follows from the classical Kepler's third law, and $n_\varphi = 1$ because the center of attraction of a Keplerian ellipse is located at one of its foci (see figure 7). For the harmonic potential, $\tau_r = \frac{\pi}{\omega}$ and $n_\varphi = \frac{1}{2}$ because harmonic ellipses are centered at their centers of attraction, see figure 7. As it is shown in appendix D, one gets

$$\mathcal{A}_r^{\text{ke}} = \frac{\mu}{\sqrt{2|\xi_k|}} - \Lambda \quad \text{and} \quad \mathcal{A}_r^{\text{ha}} = \frac{\xi_h}{2\omega} - \frac{\Lambda}{2}.$$

For the two non classical isochrones $\psi_{\text{he}}^{\text{bo}}(r) = \pm \frac{\mu}{b} \left(1 + \sqrt{1 \mp \frac{r^2}{b^2}}\right)^{-1}$, generalizing [6] p.152, we introduce $s = 1 + \sqrt{1 \mp \frac{r^2}{b^2}}$. For the Hénon potential, $s > 2$ and the PRO has $\xi_- < 0$ according to its effective potential, see sec. 2.1 p.6. In the same way, for the bounded potential, $2 > s > 0$ and its PRO has positive energy $\xi^+ > 0$. Then, for $s_p < s_a$, the radial actions are

$$\mathcal{A}_{r,\text{he}}^{\text{bo}} = \mp \frac{b\sqrt{2|\xi_\pm^+|}}{\pi} \int_{s_p}^{s_a} \frac{(s-1)}{s(s-2)} \sqrt{(s-s_p)(s_a-s)} ds$$

with

$$\begin{cases} s_p + s_a = 2 + \frac{\mu}{b|\xi_{\pm}^{\pm}|} \\ s_a s_p = \frac{4b\mu + \Lambda^2}{2b^2|\xi_{\pm}^{\pm}|}. \end{cases} \quad (53)$$

Hence, using \mathcal{I}_2 from appendix D, one gets

$$\mathcal{A}_{r,\text{he}}^{\text{bo}} = \mp \frac{\mu}{\sqrt{2|\xi_{\pm}^{\pm}|}} - \frac{1}{2} \left(\Lambda \mp \sqrt{4b\mu + \Lambda^2} \right).$$

The results follow by derivation. \square \square

The dynamics is unchanged when adding constants to potentials, i.e. $\psi \rightarrow \psi + \epsilon$. However, the expression of the periods are modified and can be deduced from propositions 4.0.1 and 4.0.2 for the reduced, physical and gauged isochrones.

Proposition 4.0.2. *Let ψ and ψ^* be two potentials related by an affine transformation $\psi^* = J_{\epsilon,\lambda}(\psi) = \psi + \epsilon + \frac{\lambda}{2r^2}$.*

An orbit defined in ψ and its affine transformation in ψ^ share the same orbital properties τ_r and n_φ .*

Provided that $\lambda + \Lambda^2 > 0$, the radial action and its derivatives are transformed as follows:

1. $\mathcal{A}_r^*(\xi; \Lambda) = \mathcal{A}_r(\xi - \epsilon; \sqrt{\lambda + \Lambda^2})$,
2. $\tau_r^*(\xi; \Lambda) = \tau_r(\xi - \epsilon; \sqrt{\lambda + \Lambda^2})$,
3. $n_\varphi^*(\xi; \Lambda) = n_\varphi(\xi - \epsilon; \sqrt{\lambda + \Lambda^2}) \frac{\Lambda}{\sqrt{\lambda + \Lambda^2}}$.

Proof. The radial action of an orbit of energy ξ and angular momentum Λ in ψ^* is given by

$$\begin{aligned} \mathcal{A}_r^*(\xi; \Lambda) &= \frac{1}{\pi} \int_{r_p^*(\xi; \Lambda)}^{r_a^*(\xi; \Lambda)} \sqrt{2(\xi - \psi^*(r)) - \frac{\Lambda^2}{r^2}} dr \\ &= \frac{1}{\pi} \int_{r_p^*(\xi; \Lambda)}^{r_a^*(\xi; \Lambda)} \sqrt{2(\xi - \epsilon - \psi(r)) - \frac{\lambda + \Lambda^2}{r^2}} dr \\ &= \frac{1}{\pi} \int_{r_p(\xi - \epsilon; \sqrt{\lambda + \Lambda^2})}^{r_a(\xi - \epsilon; \sqrt{\lambda + \Lambda^2})} \sqrt{2(\xi - \epsilon - \psi(r)) - \frac{\lambda + \Lambda^2}{r^2}} dr \\ \mathcal{A}_r^*(\xi; \Lambda) &= \mathcal{A}_r(\xi - \epsilon; \sqrt{\lambda + \Lambda^2}), \end{aligned}$$

where r is the radial distance in the reference frame associated with ψ , and r^* is the image in the same frame by the affine transformation. For the second relation we use the definition $\frac{\tau_r^*(\xi; \Lambda)}{2\pi} = \frac{\partial \mathcal{A}_r^*}{\partial \xi}(\xi; \Lambda)$. For the third one, we get

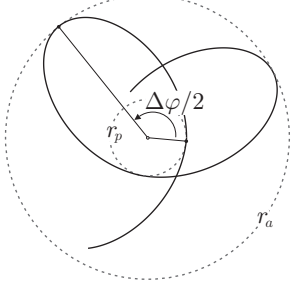
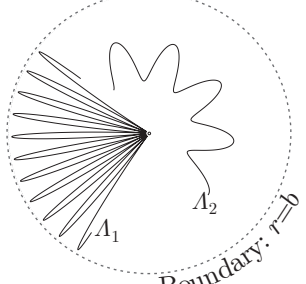
$$\begin{aligned} n_\varphi^*(\xi; \Lambda) &= -\frac{\partial \mathcal{A}_r^*}{\partial \Lambda}(\xi; \Lambda) \\ &= -\frac{\partial}{\partial \Lambda} \left(\mathcal{A}_r \left(\xi - \epsilon; \sqrt{\lambda + \Lambda^2} \right) \right) \\ &= -\frac{\partial \mathcal{A}_r}{\partial \Lambda} \left(\xi - \epsilon; \sqrt{\lambda + \Lambda^2} \right) \times \frac{\Lambda}{\sqrt{\lambda + \Lambda^2}}. \end{aligned}$$

And the third relation follows.

Eventually, a transformation $J_{\epsilon, \lambda}$ maps an orbit (ξ, Λ) onto another one of parameters $(\xi + \epsilon, \sqrt{\Lambda^2 - \lambda})$ when $\Lambda^2 - \lambda > 0$. Inserting them in the previous relations, we recover the invariance of τ_r and n_φ under $J_{\epsilon, \lambda}$: the radial period of the image orbit $\tau_r^*(\xi + \epsilon, \sqrt{\Lambda^2 - \lambda})$ is that of the primary orbit $\tau_r(\xi, \Lambda)$. In the same way, $n_\varphi^*(\xi + \epsilon; \sqrt{\Lambda^2 - \lambda}) = n_\varphi(\xi, \Lambda)$. $\square \quad \square$

Eventually, the radially periodic orbits are rosettes, [6] sect. 3. The number n_φ of revolutions to reach a periastron from the preceding one can be greater or lower than for a harmonic or Keplerian potential. A gauge introduces orbits that spiral into the origin [29], as it happens for orbits of the extremal line defining an imaginary radial distance on its parabola at the pericenter. The gauged harmonic presents a similarity with ψ_{he} and ψ_{bo} , as described in proposition 4.0.3. The precession of orbits that emerge when adding a $\frac{1}{r^2}$ -term to the potential corresponds to the one described in Proposition XLIV of Newton's *Principia* [33] for the Kepler force.

Proposition 4.0.3. *Bounded, Hénon and gauged harmonic PRO's are rosettes with azimuthal precessions n_φ such that:*

ψ_{he} and $J_{0, \lambda}(\psi_{\text{ha}})$ with $\lambda > 0$	ψ_{bo} and $J_{0, \lambda}(\psi_{\text{ha}})$ with $\lambda < 0$
$n_\varphi > 1/2$ 	$n_\varphi < 1/2$ 

Proof. Let us illustrate the case of a harmonic oscillator and its gauge transform $\psi^* = J_{0,\lambda}(\psi_{\text{ha}}) = \psi_{\text{ha}} + \frac{\lambda}{2r^2}$. From proposition 4.0.2, we get that for the modified potential,

$$\tau_r^* = \tau_r = \frac{\pi}{\omega}, \quad n_\varphi^* = \frac{\Lambda}{2\sqrt{\lambda + \Lambda^2}}.$$

Thus, for harmonic potentials, adding a gauge modifies n_φ , whereas the period never changes. Moreover we get the dynamical consequence that $n_\varphi^* < 1/2$ when $\lambda > 0$ and $n_\varphi^* > 1/2$ when $\lambda < 0$.

The parallel property exists for ψ_{he} and ψ_{bo} . According to (50) in proposition 4.0.1, $n_\varphi^{\text{bo}} = \frac{1}{2} - \frac{\Lambda}{2\sqrt{4b\mu + \Lambda^2}}$ where $\frac{\Lambda}{2\sqrt{4b\mu + \Lambda^2}} > 0$, and then $n_\varphi^{\text{bo}} < \frac{1}{2}$. In the same way, $n_\varphi^{\text{he}} > \frac{1}{2}$.

This n_φ property shapes the corresponding orbits. On the one hand, when $n_\varphi > \frac{1}{2}$, the azimuthal precession $\Delta\varphi/2$ during the transfer from apoastron ($r = r_a$) to the periastron ($r = r_p$) is greater than π . Thus the orbit must turn around the center of the system as it is indicated on the left panel of the proposition. On the other hand, when $n_\varphi < \frac{1}{2}$, the transfer $r_p \rightarrow r_a \rightarrow r_p$ cannot turn around the center; such orbits oscillate between r_a and r_p , precessing around the center, as is plotted on the right panel of the proposition. The smaller the value of the angular momentum, the tighter the oscillation is. On this right panel we have $0 \simeq \Lambda_1 < \Lambda_2$. \square \square

Let us conclude this section remarking that the extension (r_a and r_p) of an isochrone orbit is managed by its energy (see the expression of ξ in (51), (52) and (53)) when the thickness of its oscillation is governed by its angular momentum. More precisely, radial (thin) orbits are obtained when $\Lambda \rightarrow 0$ and circular (fat) orbits when $\Lambda = \Lambda_c$, the largest value possible of the angular momentum for the considered energy.

4.3 Generalization of Kepler's Third Law

The Kepler potential $\psi_{\text{ke}}(r) = -\frac{\mu}{r}$ is sourced by a point of mass M such that $\mu = GM$ where G is the Newton constant. Radially periodic orbits close after one radial period τ_r and form ellipses with semi major axes $a = -\frac{\mu}{2\xi}$. In his last major book *Harmonices Mundi* [24], Johannes Kepler proposed in 1619 his third law claiming that $\tau_r^2 \times a^{-3}$ is constant for all ellipses. Isaac Newton, half a century later, proved this empirical observation using his laws of dynamics and his gravitational force. This law appears to become a cornerstone of celestial mechanics because the Kepler constant appears to be $\tau_r^2 a^{-3} = \frac{4\pi^2}{\mu}$ and thus gives the mass of the attracting body.

In this paper we have shown that Kepler potential generates the isochrone group and we remark that Kepler's third law could be generalized. As a matter of fact, considering the specific energy ξ associated with a given PRO in an isochrone potential $\psi \in \{\psi_{\text{ke}}, \psi_{\text{he}}, \psi_{\text{bo}}\}$, we see that according to proposition 4.0.1, except for the harmonic potential, all isochrone orbits are such that

$$\tau_r^2 |\xi|^3 = \frac{\pi^2 \mu^2}{2} = \text{cst.} \quad (54)$$

Nevertheless, the law (54) expressed in terms of the specific energy is not stable under transvections of the potential, $\psi \mapsto \psi^* = \psi + \epsilon$, and has to be slightly modified for physical potentials when adding a constant. As mentioned in proposition 4.0.2, a PRO (ξ, Λ) in ψ^* will satisfy

$$\tau_r^2 |\xi - \epsilon|^3 = \frac{\pi^2 \mu^2}{2} = \text{cst.} \quad (55)$$

In these relations, ξ is the specific energy of the test particle moving on a PRO with period τ_r . The parameter μ is directly related to the total mass of the system which sources the potential when it is finite i.e. ψ_{ke} and ψ_{he} . For the other non classical isochrone ψ_{bo} , the total mass is infinite but equation (54) always holds with a less physically comprehensive μ constant. The modification of the law (54) into (55) somehow hides the symmetry of the considered system. We thus propose a geometric formulation of Kepler's Third Law for isochrones.

The formulation of Kepler $\tau_r^2 \propto a^{-3}$ in terms of the geometric parameter a is more appropriate for conveying the symmetry of the potential. In fact, the Lagrangian $L = T - U$, with T the specific kinetic energy of a particle and $U = \psi_{\text{ke}}$, is invariant, under a time $t \rightarrow \tilde{t} = \zeta t$ and space $\vec{r} \rightarrow \tilde{\vec{r}} = \varpi \vec{r}$ rescaling, if

$$\zeta^2 \propto \varpi^3$$

because ψ_{ke} is a homogeneous function of degree -1 , i.e. $\psi_{\text{ke}}(\tilde{\vec{r}}) = \varpi^{-1} \psi_{\text{ke}}(\vec{r})$. In order to geometrically express Kepler's Third law, we introduce in definition 4.1 "semi major axes", relevant to all isochrone potentials, and directly related to their Keplerian relative description. These characteristic lengths, generally related to specific energies by (51), (52) and (53), provide a method to determine the mass of an isochrone system as mentioned at the end of this section.

Definition 4.1. Let r_p and r_a be the peri- and apoastron radial distance of a given isochrone periodic orbit. We call the isochrone semi-major axis of this orbit by the following lengths:

1. in a Kepler potential,

$$a = \frac{1}{2} (r_a + r_p),$$

2. in a homogeneous box of radius R ,

$$a = \left(\frac{1}{2}\right)^{2/3} R,$$

3. in a Hénon potential,

$$a = \frac{1}{2} \left(\sqrt{b^2 + r_a^2} + \sqrt{b^2 + r_p^2} \right),$$

4. in a bounded potential,

$$a = \frac{1}{2} \left(\sqrt{b^2 - r_a^2} + \sqrt{b^2 - r_p^2} \right).$$

In definition 4.1, we have considered a homogeneous box to include the description of its elliptic trajectories with the Third Law. In fact, the situation of the harmonic potential needs more attention since ψ_{ha} is degenerate. In such a potential all test particles share the same period but different specific energies, hence relation (54) cannot hold for each specific energy.

The harmonic potential is not exactly representative of a real system because of its constant density and infinite spatial extension, which imply an infinite mass. Instead, the potential associated with a finite homogenous repartition of masses in a ball of radius R with constant density (while the outside region is empty) does represent a real system and can be written as

$$\psi_{\text{ha}}^R(r) = \begin{cases} \frac{1}{2}\omega^2 r^2 - \frac{3}{2}\omega^2 R^2 & \text{if } r < R \\ -\frac{GM}{r} & \text{if } r > R. \end{cases}$$

We call it a finite harmonic potential. Additionally, either Gauss' theorem or the continuity of the force at the boundary of the ball leads to the following relation:

$$\mu = GM = \omega^2 R^3. \tag{56}$$

As mentioned on page 22, the harmonic potential corresponds to the limit of an isochrone potential ψ_{he} or ψ_{bo} when $b \rightarrow \infty$. This result holds for the finite harmonic potential ψ_{ha}^R . In figure 13, we see the confluence of these potentials and their densities when the parameter b is large, as written in proposition 4.0.4. As it will be proven in theorem 4.1, the characteristic length for the finite harmonic also naturally appears in the expression of Kepler's Third Law.

Proposition 4.0.4. *The finite harmonic potential satisfies*

$$\psi_{\text{he}}(r) \underset{b \rightarrow \infty}{\sim} \psi_{\text{ha}}^R(r) \quad \text{and} \quad \psi_{\text{bo}}(r) \underset{b \rightarrow \infty}{\sim} \psi_{\text{ha}}^R(r) \quad \text{with} \quad R = 2^{2/3}b \quad \text{for any fixed } r.$$

Proof. As already mentioned, the potential ψ_{ha}^R is continuous in $r = R$ if and only if $\mu = GM = \omega^2 R^3$.

We assume the potentials vanish at $r = 0$ without loss of generality. We consider then the reduced potentials and their equivalents from (48) and (49) as $\psi_{\text{he}}^{\text{red}} \underset{b \rightarrow \infty}{\sim} \frac{\mu}{8b^3} r^2$ and $\psi_{\text{bo}}^{\text{red}} \underset{b \rightarrow \infty}{\sim} \frac{\mu}{8b^3} r^2$.

In this limit, the Hénon and bounded potentials behave as homogeneous spheres inside a radius $R = 2^{2/3}b$. □ □

Now, Kepler's third law can be generalized to all isochrone potentials in theorem 4.1.

Theorem 4.1. *For any radially periodic orbit in an isochrone potential, the square of the radial period is proportional to the cube of the isochrone semi-major axis by*

$$\tau_r^2 = \frac{4\pi^2}{\mu} a^3, \tag{57}$$

where μ is the mass parameter of ψ_{ke} , ψ_{he} , ψ_{bo} and $\mu = \omega^2 R^3$ for ψ_{ha}^R .

Proof. In ψ_{ke} , it is Kepler's third law. In ψ_{he} , for a PRO of energy $\xi < 0$, the radial variable s introduced in the proof of proposition 4.0.1 satisfies (53) as

$$s_a + s_p = 2 - \frac{\mu}{\xi b} = 2 + \sqrt{\left(\frac{r_a}{b}\right)^2 + 1} + \sqrt{\left(\frac{r_p}{b}\right)^2 + 1}$$

and

$$\xi = -\frac{\mu}{2a} \quad \text{with} \quad a = \frac{\sqrt{r_a^2 + b^2} + \sqrt{r_p^2 + b^2}}{2}.$$

Inserting this expression of ξ in (54) gives (57).

Similarly, in ψ_{bo} the variable s satisfies

$$s_{\min} + s_{\max} = 2 + \frac{\mu}{\xi b} = 2 + \sqrt{1 - \left(\frac{r_p}{b}\right)^2} + \sqrt{1 - \left(\frac{r_a}{b}\right)^2}$$

and

$$\xi = \frac{\mu}{2a} > 0 \quad \text{with} \quad a = \frac{1}{2} = \sqrt{b^2 - r_p^2} + \sqrt{b^2 - r_a^2}.$$

By inserting this expression in (54), we recover the law (57).

In ψ_{ha} , all orbits have the same radial period $\tau_r = \frac{\pi}{\omega}$. When a harmonic system is compacted into a ball of radius R of constant density, then $\mu = \omega^2 R^3$ according to (56). Hence, the period could be related to the radius of the ball through the relation $\tau_r = \frac{\pi}{\sqrt{\mu}} R^{3/2}$. Introducing the length $a = \left(\frac{1}{2}\right)^{2/3} R$, one has

$$\mu \tau_r^2 = 4\pi^2 a^3. \quad \square$$

□

Thus, Kepler's third law appears to be generalized through the isochrone group. Kepler's third law is mainly used for mass determination, as in, for example, the post-newtonian approximation to estimate the mass of black holes. For a Kepler potential, only one orbit is theoretically necessary to determine the mass of the central attractive body given by μ . For other isochrone potentials, using (4.1), only two orbits would be necessary to determine the parameter b and mass μ described by their isochrone potential.

4.4 The Bertrand theorem

In 1873, J. Bertrand published a fascinating theorem: *There are only two central potentials for which all orbits with an initial velocity below a certain limit are closed, namely the Keplerian and the harmonic potentials.* While this fascinating result was proved more than 140 years ago, the proof of this theorem has been retaining the attention. According to the most recent reviews [38] and works on this topic [1, chap.3], it has been proven using very different techniques: [4, 2, 25, 23, 10], using global methods, sometimes stemming from the analysis of the precession rate as initiated in proposition XLV of [33]; [9, 15, 41, 12], developing perturbative expansions; [39, 18, 37], using inverse transformations methods; [36], by searching for additional constants of motion; and [13], mainly using Birkhoff invariants along circular orbits in a generic potential. Furthermore, the original proof does not mention the case of collision orbits. We will therefore consider

the result of Bertrand's theorem under the hypotheses of orbits that are bounded in position and bounded away from 0. We propose here to show that, in fact, Bertrand's theorem is a refined property of the isochrone one.

Theorem 4.2. *In a given radial potential ψ , if all non-circular orbits that are bounded in position and bounded away from 0 are closed, then ψ is isochrone.*

Proof. In a given radial potential ψ , if all bounded and bounded away from 0 orbits are closed, the increment of the azimuthal angle $\Delta\varphi$ during the transfer from r_a to r_p is a fractional multiple of 2π , i.e. the quantity $n_\varphi = \frac{\Delta\varphi}{2\pi} \in \mathbb{Q}$. But, for a given radial potential $\psi(r)$, we have that

$$n_\varphi = -\frac{\partial \mathcal{A}_r}{\partial \Lambda} = \frac{1}{\pi} \int_{r_p}^{r_a} \frac{\Lambda}{r^2 \sqrt{2[\xi - \psi(r)] - \frac{\Lambda^2}{r^2}}} dr$$

is a continuous mapping $(\xi, \Lambda) \mapsto n_\varphi$. By continuity, because the set $\mathbb{R} \setminus \mathbb{Q}$ is dense in \mathbb{R} , one can conclude that in order to only have closed orbits, $n_\varphi = cst \in \mathbb{Q}$. In these conditions we then have

$$0 = \frac{\partial n_\varphi}{\partial \xi}.$$

This characterizes an isochrone potential according to theorem A.1 of appendix A. The potentials of the form $-\frac{\mu}{r^\alpha}$ with $\alpha > 2$ are excluded because all orbits that are bounded in position either collide at the origin or are circular. □ □

Using our study we can go further because we have obtained a geometric and algebraic description of the whole set of isochrone potentials. More specifically, we have obtained in table (50) the explicit value of n_φ for all isochrone potentials. The completeness of our description and this table enable us to claim that Bertrand's theorem is a corollary of theorem 4.2.

Corollary 4.2.1. *The Bertrand Theorem ! There are only two central potentials for which all non-circular orbits that are bounded in position and bounded away from 0 are closed, namely the Keplerian and the harmonic potentials.*

Proof. As the quantities $\frac{\Lambda}{2\sqrt{4b\mu+\Lambda^2}}$ and $\frac{\Lambda}{\sqrt{\lambda+\Lambda^2}}$ in proposition 4.0.1 and 4.0.2 cannot be rational for each value of Λ , among all isochrone potentials, only ψ_{ke} and ψ_{ha} have rational n_φ for all orbits, i.e. for all values of (ξ, Λ) . □ □

In a given potential, the fact that all bounded orbits are closed, namely Bertrand's property, is then a supplementary restriction to the isochrone one.

5 Conclusion

In this paper we have revisited the set of isochrone orbits in radial 3D potentials. These models concern self-organised radial systems with long-range interactions like gravitation or electrostatics with one kind of electric charge. Let us summarize the main results we have obtained:

1. We have clarified the original proof by Michel Hénon [20] that isochrone potentials are contained in a branch of a parabola in adapted coordinates (theorem B.1). These parabolas characterize the property of isochrony.
2. Taking into account very general properties of potentials in physics — i.e. invariance under the addition of a constant, conservation of the energy and angular momentum for isolated radial systems — we have given a geometrical characterization and classification of the set of all isochrone orbits/potentials that we have completed. This characterization (theorem 2.5) is based on a subgroup \mathbb{A} of the real affine group.
3. We have shown (theorem 2.5 and sec. 2.5) that under the group action of \mathbb{A} , any isochrone potential is in the orbit of one of the four fundamental potentials: Kepler, Hénon, Bounded or Harmonic (definition 2.2).
4. Focusing on orbits, we have proposed a mapping which generalizes the Bohlin transformation to all isochrone potentials. This mapping, summarized in theorem 3.1, connects any Keplerian elliptic orbit to a particular isochrone radially periodic orbit. Reciprocally, by theorem 3.2, we have shown how to construct the elliptic Keplerian orbit connected to any isochrone periodic orbit. This mapping is based on a particular linear transformation, that we call a bolst, which preserves the orbital differential equation for a given value of the angular momentum.
5. With the set of symmetric bolsts, namely Ibolsts, we have revealed the relative behavior of the isochrone property of orbits/potentials.

We have detailed in sec. 3.2 a lot of similarities between the special theory of relativity and the isochrony of orbits in radial potentials. In this view, a given orbit in an isochrone potential is seen as a Keplerian orbit in its special frame. This is the Isochrone Relativity presented in sec. 3.2. The time and energy are relative to each orbit which defines a frame of reference. Various examples were presented and illustrated to construct isochrone orbits in isochrone potentials.

6. The explicit expression of the radial (τ_r) and azimuthal (n_φ) periods was calculated for all fundamental isochrone potentials. These results are presented in proposition 4.0.1. The computation of these periods in physical or gauged isochrones is possible using the results presented in proposition 4.0.2.
7. We have proposed a generalization of the quadricentennial Kepler's Third Law in theorem 4.1. While this classic law involves the semi major axis of *closed* Keplerian orbits, we define characteristic lengths in each isochrone potential that are related to the radial period in the famous $3/2$ power equation. This rational value $3/2$ is well known to be related to the mechanical similarity involved in the Kepler potential and its -1 homogeneity property (e.g. [26] p. 22-24). In this view, the generalization of the Kepler's Third Law to any isochrone is not surprising since we have seen that any isochrone is a Kepler in the adequate referential.
8. Noting that both the radial period τ_r and the precession rate n_φ are partial derivatives of the same quantity, i.e. the radial action \mathcal{A}_r , we observed that the famous Bertrand's theorem is a specific property of isochrones. Once again this property could be interpreted as a consequence of the isochrone relativity.

The essence of isochrony is Keplerian. As isochrony is characterized by the parabolic property in Hénon's variables, we understand the linear transformations that act on these parabolas and are shaped by the bolst $B_{\alpha,\beta}$ play crucial roles. Merging these ideas, we conjecture that a theory of general relativity of radial potentials could be formulated using non-linear transformations. This theory could relate any orbit in a radial potential to an associated orbit in a Kepler potential.

In a forthcoming paper we will explain the physical importance of the isochrone potential during the formation and evolution process of self-gravitating systems.

Appendix

A Isochrone characterization

Let us recall that the radial action \mathcal{A}_r gives the radial period τ_r and the increment of the azimuthal angle n_φ through (3) and (4) in sec. 2.1:

$$\frac{\partial \mathcal{A}_r}{\partial \xi} = \frac{\tau_r}{2\pi} \quad \text{and} \quad -\frac{\partial \mathcal{A}_r}{\partial \Lambda} = \frac{\Delta\varphi}{2\pi} = n_\varphi.$$

The exclusive ξ -dependency of τ_r is the fundamental isochrone property used by Michel Hénon to define isochrone potentials. After his analysis, he remarked the exclusive Λ -dependency of n_φ for his potential. The following theorem establishes the equivalence of properties which can characterize isochrone potentials as a whole.

Theorem A.1. *Consider a central potential ψ . Then the following properties are equivalent:*

1. *For any orbit (ξ, Λ) in ψ , τ_r only depends on ξ .*
2. *For any orbit (ξ, Λ) in ψ , n_φ only depends on Λ .*
3. *There exist two function f and g such that for any (ξ, Λ) the radial action is $\mathcal{A}_r(\xi, \Lambda) = f(\xi) + g(\Lambda)$.*

Proof. The separation of variables in the radial action expressed in 3 implies the two properties 1 and 2 by direct differentiation with respect to ξ for 1 and Λ for 2.

Assume 2 is true for any orbit in the central potential ψ . Then $\frac{\partial \mathcal{A}_r}{\partial \xi} = \frac{\tau_r(\xi)}{2\pi}$ and by integration there exists a function g , constant with respect to ξ , such that $\mathcal{A}_r(\xi, \Lambda) = f(\xi) + g(\Lambda)$, where f is a primitive of $\frac{\tau_r}{2\pi}$. We thus recover 3. In the same way, assuming 2 implies 3. \square \square

B Proof of a parabola property

Michel Hénon has shown in [20] the equivalence between the isochrony of a potential ψ and the parabolic property of the graph \mathcal{C} of $f : x \rightarrow x\psi$ associated with it. We propose here a different proof based on the analyticity of the potential.

We call (\mathcal{P}) this parabolic property, and it can be formulated as follows. A function $f : I \rightarrow \mathbb{R}$ has the property (\mathcal{P}) if and only if :

1. f is either convex or concave on the real interval I , i.e. $f'' > 0$ or $f'' < 0$ on I .
2. For any P_0 belonging to its graph \mathcal{C} , and for any line \mathcal{L} parallel to the tangent $\mathcal{T}_{P_0}(\mathcal{C})$, the square length of the projected chord $|x_{a,1} - x_{p,1}|$ is proportional to the distance between the chord and the tangent to the curve that is parallel to the chord. The proportional relation holds equivalently with the vertical distance P_0I between $\mathcal{T}_{P_0}(\mathcal{C})$ and \mathcal{L} . In figure 2 we have $\mathcal{T}_{P_0}(\mathcal{C}) : y = \xi x - \Lambda_0^2$ and $\mathcal{L} : y = \xi x - \Lambda_1^2$.

In terms of function, this last point translates as follows:

$$(\mathcal{P}) : \begin{cases} \forall x_0 \in I, \exists \varpi(x_0) \in \mathbb{R}_+ \text{ such that } \forall \lambda > 0, \text{ when they exist,} \\ \text{the two solutions } x_p \text{ and } x_a \text{ of the equation} \\ f(x) - f(x_0) = \lambda + f'(x_0)(x - x_0) \\ \text{satisfy the relation } (x_a - x_p) = \varpi(x_0)\sqrt{\lambda} \text{ with } x_a > x_p. \end{cases}$$

Michel Hénon's equivalence then corresponds to the following theorem.

Theorem B.1. *Let $f : I \rightarrow \mathbb{R}$ be an analytic real function on an interval $I \subset \mathbb{R}$. Then the graph of f is a parabola if and only if f has the property (\mathcal{P}) .*

The proof of this result will be done in several steps. The first one is a reduction procedure given by the following lemma.

Lemma B.2. *Let $g : I \rightarrow \mathbb{R}$ be a real analytic function satisfying property (\mathcal{P}) . Then we have*

1. *For any real constant $a \neq 0$, $f := ag$ satisfies (\mathcal{P}) ;*
2. *For any constants $(\varepsilon, \lambda) \in \mathbb{R}^2$, $f(x) = g(x) + \varepsilon x + \lambda$ satisfies (\mathcal{P}) ;*
3. *For any constants $(\varepsilon, \lambda) \in \mathbb{R}^2$, with $\varepsilon \neq 0$, $f(x) := g(\varepsilon x + \lambda)$ satisfies (\mathcal{P}) .*

This statement indicates that property (\mathcal{P}) is stable by affine transformations acting on the graph of the considered function. Its proof is quite obvious and is left to the reader.

Any graph of a parabola can be obtained by the transformations of lemma B.2 of the graphs of $x \mapsto \sqrt{x}$ or $x \mapsto x^2$. It follows that, if the graph of f is a parabola, then f satisfies the simple implication of the theorem.

In order to have the converse implication, i.e. $(\mathcal{P}) \implies \mathcal{C}$ is a parabola, we now consider the simple case where, in figure 2, $\mathcal{T}_{P_0}(\mathcal{C})$ is horizontal.

Lemma B.3. *If $\varphi : I \rightarrow \mathbb{R}$ is a real analytic function and if at $x_0 \in I$ we have $\varphi'(x_0) = 0$ and $\varphi''(x_0) = 2$, then*

$$5 \left[\varphi^{(3)}(x_0) \right]^2 = 6\varphi^{(4)}(x_0). \quad (\text{B1})$$

Proof. Let $\varphi(x) = g(z)$ with $z = x - x_0$. Then, since φ is analytic, g has a convergent Taylor expansion at x_0 of the form $g(z) = z^2 + g_3z^3 + g_4z^4 + \dots$, such that

$$g(z) = z^2 \left(1 + \sum_{n \geq 3} g_n z^{n-2} \right) = z^2(1 + R(z)),$$

where $R(z)$ is a convergent series that vanishes at $z = 0$. Then, we may expand

$$\sqrt{1 + R(z)} = 1 + \frac{1}{2}R + \frac{1}{2!} \left(\frac{1}{2} \right) \left(\frac{1}{2} - 1 \right) R^2 + \dots$$

and insert it in

$$\sqrt{g(z)} = G(z) = z\sqrt{1 + R(z)} = z + G_2z^2 + G_3z^3 + \dots$$

Because $G(0) = 0$ and $G'(0) = 1$, G is locally bijective in the neighborhood of $z = 0$; the analytic inverse function theorem assures that its inverse H is also a convergent power series $H(z) = z + \sum_{n \geq 2} h_n z^n$.

The fact that φ satisfies (\mathcal{P}) means that for any small enough $\lambda > 0$ the two solutions z_1 and $z_2 > z_1$ of $g(z) = \lambda$ satisfy $z_2 - z_1 = \varpi(x_0)\sqrt{\lambda}$. However,

$$\begin{aligned} g(z) = \lambda &\Leftrightarrow G^2(z) = \lambda \\ &\Leftrightarrow G(z) = \pm\lambda \\ &\Leftrightarrow z = H(\pm\lambda). \end{aligned}$$

More precisely, $z_2 = H(\sqrt{\lambda})$ and $z_1 = H(-\sqrt{\lambda})$ if $\lambda \geq 0$ is small enough because H locally increases. The second condition from (\mathcal{P}) gives $H(\sqrt{\lambda}) - H(-\sqrt{\lambda}) = \varpi(x_0)\sqrt{\lambda}$ for sufficiently small $\lambda \geq 0$ and

$$H(t) - H(-t) = \varpi t, \quad (\text{B2})$$

since all members of the previous equation are power series. Inserting the expression of $H(t) = \sum_{n \geq 1} h_n t^n$ in (B2), noting that the even terms disappear, one finds $2h_1 = 2 = \varpi$ and $h_{2m+1} = 0$ if $m \geq 1$. In other words,

$$H(t) = t + h_2 t^2 + h_4 t^4 + \dots$$

Identifying the terms of the equality given by $H \circ G(z) = z$, one specifically finds $G_2 = -h_2$ and $G_3 = -2h_2G_2 = 2h_2^2$. Hence the expansion of g is written as

$$\begin{aligned} g(z) = G^2(z) &= z^2 - 2h_2z^3 + 5h_2^2z^4 + \dots \\ &= \frac{1}{2}g''(x_0)z^2 + \frac{1}{6}g^{(3)}(x_0)z^3 + \frac{1}{24}g^{(4)}(x_0)z^4 + \dots, \end{aligned}$$

where the identification between each term leads to $(g^{(3)}(x_0))^2 = 12^2h_2^2 = \frac{6}{5}g^{(4)}(x_0)$ which is exactly (B1). \square \square

We now exploit this particular case to characterize the property (\mathcal{P}) in terms of a differential equation.

Lemma B.4. *Let $f : I \rightarrow \mathbb{R}$ be a real analytic function satisfying (\mathcal{P}) . Then f also satisfies*

$$\forall x_0 \in I, 5 \left[f^{(3)}(x_0) \right]^2 = 3f^{(4)}(x_0) f''(x_0). \quad (\text{B3})$$

Proof. For any point $x_0 \in I$ with $f''(x_0) \neq 0$, the function

$$\varphi(x) = \frac{2}{f''(x_0)} [f(x) - f(x_0) - f'(x_0)(x - x_0)]$$

satisfies the property (\mathcal{P}) according to lemma B.2. Moreover we have that $\varphi'(x_0) = 0$ and

$$\begin{cases} \varphi''(x) = \frac{2f''(x)}{f''(x_0)} \implies \varphi''(x_0) = 2 \\ \varphi^{(3)}(x) = \frac{2f^{(3)}(x)}{f''(x_0)} \implies \varphi^{(3)}(x_0) = \frac{2f^{(3)}(x_0)}{f''(x_0)} \\ \varphi^{(4)}(x) = \frac{2f^{(4)}(x)}{f''(x_0)} \implies \varphi^{(4)}(x_0) = \frac{2f^{(4)}(x_0)}{f''(x_0)}. \end{cases}$$

As a consequence, φ satisfies the assumptions of lemma B.3 and therefore (B1) \implies (B3). \square \square

Let us observe that (B3) was obtained under the condition that $f''(x_0) \neq 0$. By analytic continuation the relation is still satisfied at the isolated points where f'' could vanish.

We are therefore led to solve (B3), which is in fact the *universal differential equation for parabolas*. Setting $w = f''$, (B3) becomes

$$5(w')^2 = 3w''w. \quad (\text{B4})$$

Two cases may occur:

1. If $w' = f^{(3)} := 0$ on I :
then f'' is constant and f is a second-degree polynomial and its graph \mathcal{C} is a parabola.
2. If $w' = f^{(3)}$ do not vanish everywhere on I :
then on any subset where $w' \neq 0$, equation (B4) becomes

$$\frac{5w'}{w} = \frac{3w''}{w'},$$

which gives by integration

$$5 \ln |w| = 3 \ln |w'| + cst \implies w'w^{-5/3} = cst.$$

Hence $w^{-2/3}$ is a linear function of x , namely $w(x) = f''(x) = (\varepsilon x + \lambda)^{-3/2}$. By integrating this equation twice, we get that f is proportional to $f_0(x) = \sqrt{\varepsilon x + \lambda} + ax + b$ whose graph is a parabola too.

This concludes the proof of theorem B.1.

C Useful Lemmas

Consider

- a frame $\mathcal{R}_O = (O, \vec{i}, \vec{j})$ with coordinates (x, y) for each point M ;
- a linear application $L : \mathbb{R}^2 \rightarrow \mathbb{R}^2$ such that $L(\vec{i}) = \vec{u}$ and $L(\vec{j}) = \vec{v}$;
- a curve \mathcal{C} of equation $f(x, y) = 0$ in the frame \mathcal{R} .

The linearity of L ensures the two properties below.

Lemma C.1. *The cartesian equation of curve $\mathcal{C}' = L(\mathcal{C})$ in the frame $\mathcal{R}'_O = (O, \vec{u}, \vec{v})$ remains $f(x, y) = 0$.*

Proof. Consider $\overrightarrow{OM} = x\vec{i} + y\vec{j}$. Then $M \in \mathcal{C} \Leftrightarrow f(x, y) = 0$. But $L(\overrightarrow{OM}) = xL(\vec{i}) + yL(\vec{j}) = x\vec{u} + y\vec{v} \in \mathcal{C}'$ by definition. Thus $f(x, y) = 0$ also defines \mathcal{C}' in \mathcal{R}'_O . \square

Define

- $\mathcal{T}_O(\mathcal{P})$ the tangent at the origin O to a parabola \mathcal{P} ;

- $\mathcal{S}(\mathcal{P})$ the symmetry axis of parabola \mathcal{P} .

Then we have the following lemma:

Lemma C.2. *If $\mathcal{P}' = L(\mathcal{P})$ then $\mathcal{T}_O(\mathcal{P}') = L(\mathcal{T}_O(\mathcal{P}))$ and $\mathcal{S}(\mathcal{P}') = L(\mathcal{S}(\mathcal{P}))$.*

Proof. According to lemma C.1, \mathcal{P} and \mathcal{P}' have the equation $(ax + by) + e = (cx + dy)^2$ in their respective frames. Then the tangent \mathcal{T}_O has the direction vector $\vec{t} = -b\vec{i} + a\vec{j}$ and the symmetry axis $\mathcal{S}(\mathcal{P})$ has the vector $\vec{n} = -d\vec{i} + c\vec{j}$. In the same way, with natural notations, $\vec{t}' = -b\vec{u} + a\vec{v}$ and $\vec{n}' = -d\vec{u} + c\vec{v}$. Thus $\vec{t}' = L(\vec{t})$ and $\vec{n}' = L(\vec{n})$. \square

D Isochrone integrals

Lemma D.1. *The Keplerian and harmonic radial actions are given by*

$$\mathcal{A}_r^{\text{ke}} = \frac{\mu}{\sqrt{-2\xi}} - \Lambda \quad \text{and} \quad \mathcal{A}_r^{\text{ha}} = \frac{\xi}{2\omega} - \frac{\Lambda}{2}.$$

For any pair of positive real (u_1, u_2) such that $u_1 < u_2$, we have

$$\mathcal{I}_1(u_1, u_2) = \int_{u_1}^{u_2} \frac{\sqrt{(u - u_1)(u_2 - u)}}{u} du = \frac{\pi}{2} (u_1 + u_2 - 2\sqrt{u_1 u_2})$$

and

$$\begin{aligned} \mathcal{I}_2(u_1, u_2) &= \int_{u_1}^{u_2} \frac{(u - 1) \sqrt{(u - u_1)(u_2 - u)}}{u(u - 2)} du \\ &= \begin{cases} \frac{\pi}{2} \left[u_1 + u_2 - \sqrt{u_1 u_2} - \sqrt{(u_1 - 2)(u_2 - 2)} - 2 \right] & \text{if } 2 < u_1 \\ \frac{\pi}{2} \left[u_1 + u_2 - \sqrt{u_1 u_2} + \sqrt{(u_1 - 2)(u_2 - 2)} - 2 \right] & \text{if } u_2 < 2. \end{cases} \end{aligned}$$

The result of \mathcal{I}_1 can be obtained by a direct meticulous computation; instead, we propose to deduce it from the physical computation of the Keplerian radial action.

In a second step, we will deduce \mathcal{I}_2 from \mathcal{I}_1 .

D.1 Computation of $\mathcal{A}_r^{\text{ke}}$, $\mathcal{A}_r^{\text{ha}}$ and physical deduction of \mathcal{I}_1

The radial action for an orbit of negative energy ξ and momentum Λ in a Keplerian potential $\psi_{\text{ke}}(r) = -\frac{\mu}{r}$ is given by

$$\mathcal{A}_r^{\text{ke}} = \frac{1}{\pi} \int_{r_p}^{r_a} \sqrt{2[\xi - \psi_{\text{ke}}(r)] - \frac{\Lambda^2}{r^2}} dr \quad (\text{D5})$$

$$= \frac{\sqrt{-2\xi}}{\pi} \int_{r_p}^{r_a} \frac{\sqrt{(r-r_p)(r_a-r)}}{r} dr \quad \text{with} \quad \begin{cases} r_p + r_a = -\frac{\mu}{\xi} \\ r_p r_a = -\frac{\Lambda^2}{2\xi} \end{cases} \quad (\text{D6})$$

as in (51). The radial period and the azimuthal precession are just partial derivatives of the radial action according to (3) and (4):

$$\frac{\partial \mathcal{A}_r}{\partial \xi} = \frac{\tau_r}{2\pi} \quad \text{and} \quad \frac{\partial \mathcal{A}_r}{\partial \Lambda} = -\frac{\Delta\varphi}{2\pi} = -n_\varphi.$$

For a negative energy, the Kepler orbit is an ellipse with semi-major axis $a = \frac{1}{2}(r_a + r_p)$, where r_a and r_p are respectively the apoastron and the periastron of the trajectory (hence $r_a \geq r_p$). For this Keplerian ellipse we trivially have $\Delta\varphi = 2\pi$ and then $n_\varphi = 1$. By integration, one gets in this case

$$\frac{\partial \mathcal{A}_r^{\text{ke}}}{\partial \Lambda} = -1 \quad \implies \quad \mathcal{A}_r^{\text{ke}} = -\Lambda + f(\xi).$$

The unknown function $f(\xi)$ could be expressed in terms of the radial period through the relation

$$\tau_r = 2\pi \frac{\partial \mathcal{A}_r^{\text{ke}}}{\partial \xi} = 2\pi f'(\xi).$$

From the classical Kepler's third law, we have $\tau_r = \frac{\pi\mu}{\sqrt{2(-\xi)^{3/2}}}$, which gives

$$f(\xi) = \frac{\mu}{2\sqrt{2}} \int (-\xi)^{-3/2} d\xi + c = \frac{\mu}{\sqrt{-2\xi}} + c \quad \implies \quad \mathcal{A}_r^{\text{ke}} = \frac{\mu}{\sqrt{-2\xi}} - \Lambda + c, \quad (\text{D7})$$

where c is a constant. On the one hand, for a circular Keplerian orbit we have $r_a = r_p$, so that $\mathcal{A}_r^{\text{ke}}$ given by (D6) vanishes in this case. On the other hand, a circular Keplerian orbit is characterized by $\Lambda = \frac{\mu}{\sqrt{-2\xi}}$. Combining these two remarks in (D7) gives $c = 0$. Plugging this result into (D6), one obtains

$$\mathcal{I}_1(r_p, r_a) = \frac{\pi}{\sqrt{-2\xi}} \mathcal{A}_r^{\text{ke}} = \frac{\pi}{2} \left(\frac{\mu}{(-\xi)} - \frac{2\Lambda}{\sqrt{-2\xi}} \right), \quad (\text{D8})$$

where we recognize the values of the sum and the product of r_a and r_p given by (D6). Hence,

$$\mathcal{I}_1(r_p, r_a) = \frac{\pi}{2} (r_p + r_a - 2\sqrt{r_p r_a}).$$

Since the above formula holds for any arbitrary positive numbers $r_p \leq r_a$, we deduce the explicit expression of \mathcal{I}_1 given in the lemma.

In the same way, given $\tau_r = \frac{\pi}{\omega}$ and $n_\varphi = \frac{1}{2}$ to compute the radial action with (3) and (4), the proof can be done similarly for a harmonic potential.

D.2 Proof for the expression of \mathcal{I}_2

The result for $\mathcal{I}_2(u_1, u_2)$ simply comes from the relation

$$\frac{2(u-1)}{u(u-2)} = \frac{1}{u} + \frac{1}{u-2}$$

from which we have

$$2\mathcal{I}_2(u_1, u_2) = \mathcal{I}_1(u_1, u_2) + \int_{u_1}^{u_2} \frac{\sqrt{(u-u_1)(u_2-u)}}{u-2} du. \quad (\text{D9})$$

Two cases are of interest:

1. If $2 < u_1 < u_2$, then plugging $v = u - 2$ into the last integral of (D9), we get $2\mathcal{I}_2(u_1, u_2) = \mathcal{I}_1(u_1, u_2) + \mathcal{I}_1(u_1 - 2, u_2 - 2)$ which gives

$$\mathcal{I}_2(u_1, u_2) = \frac{\pi}{2} \left[u_1 + u_2 - \sqrt{u_1 u_2} - \sqrt{(u_1 - 2)(u_2 - 2)} - 2 \right].$$

2. If $0 < u_1 < u_2 < 2$, then plugging $v = 2 - u$ into the last integral of (D9), we get $2\mathcal{I}_2(u_1, u_2) = \mathcal{I}_1(u_1, u_2) - \mathcal{I}_1(2 - u_1, 2 - u_2)$ which gives

$$\mathcal{I}_2(u_1, u_2) = \frac{\pi}{2} \left[u_1 + u_2 - \sqrt{u_1 u_2} + \sqrt{(u_1 - 2)(u_2 - 2)} - 2 \right].$$

This completes the proof for \mathcal{I}_2 .

Acknowledgment This work is supported by the ‘‘IDI 2015’’ project funded by the IDEX Paris-Saclay, ANR-11-IDEX-0003-02. JP especially thanks Jean-Baptiste Fouvry for helpful discussions about Bertrand’s theorem. ASP especially thanks Alain Albouy for his great remarks on Bertrand’s theorem and for sharing his deep historical knowledge. The authors are grateful to Faisal Amlani for his detailed copy-editing of the paper and thank the referees of the article for their helpful comments and fruitful suggestions.

References

- [1] Albouy A., Lectures on the two-body problem, Classical and celestial mechanics (Recife, 1993/1999), pp.63-116, 2002
- [2] Arnold V. I., Mathematical Methods of Classical Mechanics, Springer-Verlag, New York, 1978
- [3] Arnold V.I., Huygens & Barrow & Newton & Hooke, Birkhäuser Verlag, Basel, p.95, 1990
- [4] Bertrand J., Théorème relatif au mouvement d'un point attiré vers un centre fixe. Comptes Rendus de l'Académie des Sciences de Paris, 77, p. 849–853, 1873
- [5] Binney J., Hénon's Isochrone Model, in “Une vie dédiée aux systèmes dynamiques” ed. J.-M. Alimi, R. Mohayaee & J. Perez, Hermann, 2016, p.99–109 - arxiv astro-ph 1411.4937
- [6] Binney J., Tremaine S., Galactic Dynamics 2nd edition, Princeton University Press, 2008
- [7] Bohlin K., Bull. Astron. Ser. I, 28, 113, 1911
- [8] Borel E., Introduction géométrique à quelques théories physiques, Gauthier-Villars, 1914
- [9] Brown L. S., Forces giving no orbit precession, Am. J. Phys. 46, p. 930–931, 1978
- [10] Castro-Quilantan J. L., Del Rio-Correa J. L. & Medina M. A. R., Alternative proof of Bertrand's theorem using a phase space approach, Rev. Mex. Fis., 42, p. 867–877, 1996
- [11] Denhen W., A Family of Potential-Density Pairs for Spherical Galaxies and Bulges, Mon. Not. R. Astron. Soc, 265, p.250, 1993
- [12] Fasano A. & Marni S., Analytic Mechanics - An Introduction, Oxford University Press, Oxford England, 2006
- [13] Féjoz, J., Kaczmarek, L., Sur le théorème de Bertrand (d'après Michael Herman), Michael Herman Memorial Issue, Ergodic Theory Dyn. Sys.24:5, 15831589, 2004

- [14] Gidas B., Ni W.-M., Nirenberg L., Symmetry of positive solutions of nonlinear elliptic equations in \mathbb{R}^n , *Math. Analysis & App.*, 79, pp. 369-402, 1981
- [15] Goldstein H., *Classical Mechanics*, Addison Wesley, New York, p. 601–605, 1981
- [16]ourgoulhon, E., *Special Relativity in General Frames, Graduate Texts in Physics*, Springer, 784 pages, 2013
- [17] Goursat E., Les transformations isogonales en Mécanique, *Comptes rendus hebdomadaires de l'académie des sciences*, 108, pp. 446-448, 1889
- [18] Grandati Y., Bérard A. & Ménas F., Inverse problem and Bertrand's theorem, *Am. J. Phys.* 76, p. 782–787, 2008
- [19] Grandati Y., Berard A., and Mohrbach H., Complex representation of planar motions and conserved quantities of the Kepler and Hooke problems. *Journal of Nonlinear Mathematical Physics*, Vol.17, No. 2, 213-225, 2010
- [20] Hénon M., L'amas isochrone, *Annales d'Astrophysique*, Vol. 22, p.126, 1959
- [21] Hernquist L., An analytical model for spherical galaxies and bulges, *Ap. J.*, . 356, pp. 359-364, 1990
- [22] Jaffe W., A simple model for the distribution of light in spherical galaxies, *Mon. Not. R. Astron. Soc*, 202, p.995–999, 1983
- [23] Jovanović V., A note on the proof of Bertrand's theorem, *Theoretical and Applied Mathematics*, Vol. 42, Issue 1, pp.27-33, 2015
- [24] Kepler J., *Harmonices Mundi*, 1619
- [25] Lagrange J.-L., *Solution de différents problèmes de calcul intégral, Œuvres complètes*, Vol. I, p.573
- [26] Landau L.D., Lifshitz E.M., *Mechanics - Volume 1 of A Course of Theoretical Physics*, Pergamon Press, 1969
- [27] Levi-Civita T., Sur la résolution qualitative du problème restreint des trois corps, *Acta Math.*, 30, 1906

- [28] Lynden-Bell D., Statistical mechanics of violent relaxation in stellar systems, *Mon. Not. R. Astron. Soc*, 136,p.101,1967
- [29] Lynden-Bell, D., Bound central orbits, *Mon. Not. R. Astron Soc*, 447 (2): 1962-1972, 2015
- [30] Lynden-Bell D., Variations on the theme of Michel Hénon's Isochrone, in "Une vie dédiée aux systèmes dynamiques" ed. J.-M. Alimi, R. Mohayaee & J. Perez, Hermann, 2016, p.81–86 - arxiv astro-ph 1411.4926
- [31] Lynden-Bell D., Jin S., Analytic central orbits and their transformation group, *Mon. Not. R. Astron. Soc*, 386, pp. 245-260, 2008
- [32] MacLaurin C., A treatise on fluxions, London : W. Baynes, 1801
- [33] Newton I., *Philosophiae naturalis principia mathematica*, London, 1756
- [34] Navarro J., Frenk C., White S., The Structure of Cold Dark Matter Halos, *Ap.J*, 463, p. 563, 1996
- [35] Perez J., Aly J.-J., Stability of spherical self-gravitating systems I: Analytical results, *Mon. Not. R. Astron. Soc*, 280, p. 689, 1996
- [36] Rartinez-y-Romero R. P., Nunez-Yepez H. N. & Salas-Brito A. L., Closed orbits and constants of motion in classical mechanics, *Eur. J. Phys.* 13, p. 26–31, 1992
- [37] Santos F., Soares V. & Tort A., Determination of the Apsidal Angle and Bertrand's theorem, *Phys. Rev. E*, 79, 036605-1–6, 2009
- [38] Siu A. Chin, A truly elementary proof of Bertrand's theorem, *Am. J. Phys.* , 83, 2015
- [39] Tikochinsky Y., A simplified proof of Bertrand's theorem, *Am. J. Phys.* 56, p.1073–1075, 1988
- [40] de Vaucouleurs G., Recherches sur les Nebuleuses Extragalactiques, *Ann. Astroph.*, 11, p.247, 1948
- [41] Zarmi Y., The Bertrand theorem revisited, *Am. J. Phys.* 70, p. 446–449, 2002